

PREPARATION AND CHARACTERIZATION OF ALKYD  
COATING WITH SELF-HEALING ABILITY

NORNADILA BINTI MOHD SAMAN

FACULTY OF SCIENCE  
UNIVERSITY OF MALAYA  
KUALA LUMPUR

2019

**PREPARATION AND CHARACTERIZATION OF  
ALKYD COATING WITH SELF HEALING ABILITY**

**NORNADILA BINTI MOHD SAMAN**

**DISSERTATION SUBMITTED IN FULFILMENT OF  
THE REQUIREMENTS FOR THE DEGREE OF MASTER  
OF SCIENCE**

**DEPARTMENT OF CHEMISTRY  
FACULTY OF SCIENCE  
UNIVERSITY OF MALAYA  
KUALA LUMPUR**

**2019**

**UNIVERSITY OF MALAYA**  
**ORIGINAL LITERARY WORK DECLARATION**

Name of Candidate: Nornadila binti Mohd Saman

Matric No: SGR150060

Name of Degree: Master of Science

Title of Project Paper/Research Report/Dissertation/Thesis ("this Work"):

Preparation and Characterization of Alkyd Coating with Self-Healing

Ability Field of Study:

Polymer Chemistry

I do solemnly and sincerely declare that:

- (1) I am the sole author/writer of this Work;
- (2) This Work is original;
- (3) Any use of any work in which copyright exists was done by way of fair dealing and for permitted purposes and any excerpt or extract from, or reference to or reproduction of any copyright work has been disclosed expressly and sufficiently and the title of the Work and its authorship have been acknowledged in this Work;
- (4) I do not have any actual knowledge nor do I ought reasonably to know that the making of this work constitutes an infringement of any copyright work;
- (5) I hereby assign all and every rights in the copyright to this Work to the University of Malaya ("UM"), who henceforth shall be owner of the copyright in this Work and that any reproduction or use in any form or by any means whatsoever is prohibited without the written consent of UM having been first had and obtained;
- (6) I am fully aware that if in the course of making this Work I have infringed any copyright whether intentionally or otherwise, I may be subject to legal action or any other action as may be determined by UM.

Candidate's Signature

Date:

Subscribed and solemnly declared before,

Witness's Signature

Date:

Name:

Designation:

# PREPARATION AND CHARACTERIZATION OF ALKYD COATING WITH SELF-HEALING ABILITY

## ABSTRACT

Apart from decorative purposes, coatings have also been applied to metal surface to inhibit corrosion by protecting the substrate from environmental exposure. This work focuses on the use of UV-curable palm oil-based alkyd for surface coating application. This type of coating is a form of environmentally friendly coating that involves low, if any, emission of volatile organic compounds (VOCs) during curing. Nonetheless, UV-cured alkyd coating is just similar to any other coatings, where it is vulnerable to damages such as formation of microcracks during its service. By introducing self-healing properties into the alkyd coating, it can avoid further catastrophic failure and prolong the lifespan of the coating and its substrate. One of the objectives of this study is to introduce self-healing ability to the alkyd coating. Self-healing alkyd coating consists of microcapsules containing healing agent, implanted into alkyd coating matrix. Alkyd was synthesized as a binder in this coating mixture while methyl methacrylate (MMA) serves as reactive diluents and benzophenone as UV-photoinitiator. Diglycidyl ether bisphenol-A based epoxy (EPON828) and pentaerythritol tetrakis (3-mercaptopropionate) (PETMP) were chosen as the healing agents and microencapsulated by in situ polymerization. Self-healing process of the coating took 10 minutes after the coating was intentionally scratched. The efficacy of the self-healing ability of the coating was investigated using high powered microscope and potentiodynamic polarization. The coating showed excellent corrosion resistance and recorded good film properties.

**Keywords:** Self-healing coating; UV-curing; alkyd coating; microcapsule; palm oil

# **PENYEDIAAN DAN PENCIRIAN SALUTAN ALKID DENGAN KEUPAYAAN SWA PULIH**

## **ABSTRAK**

Selain daripada hiasan, salutan juga telah digunakan pada permukaan logam untuk menghalang kakisan dengan melindungi substrat daripada pendedahan alam sekitar. Kerja ini memberi tumpuan kepada penggunaan silang kait UV alkid berasaskan minyak sawit untuk digunakan sebagai aplikasi permukaan salutan. Salutan ini merupakan satu bentuk salutan mesra alam yang mengurangkan pelepasan sebatian organik meruap (VOC) jika ada, semasa proses silang kait. Walau bagaimanapun, salutan silang kait UV alkid sama juga seperti salutan yang lain, di mana ia terdedah kepada kerosakan seperti pembentukan keretakan mikro semasa tempoh penggunaannya. Dengan memperkenalkan sifat swasembuh ke dalam salutan alkid, ia dapat mengelakkan kegagalan yang lebih teruk dan seterusnya dapat memanjangkan jangka hayat salutan dan substratnya. Salah satu objektif kajian ini adalah untuk memperkenalkan keupayaan swasembuh ke dalam salutan alkid. Salutan alkid swasembuh terdiri daripada mikrokapsul yang mengandungi agen penyembuhan, yang dibenamkan ke dalam matriks salutan alkid. Alkid disintesis sebagai pengikat dalam campuran salutan ini sementara metil metakrilat (MMA) pula bertindak sebagai pelarut reaktif dan benzofenon sebagai UV-fotoinisiator. Epoksi berasaskan bisfenol-A diglisidil eter (EPON828) dan pentaeritritol tetrakis (3-merkaptopropionat) (PETMP) dipilih sebagai agen penyembuhan dan pemikrokapsulan oleh pempolimeran 'in situ'. Proses swasembuh oleh salutan berlaku dalam masa 10 minit selepas salutan itu dicalarkan dengan sengaja. Keberkesanan keupayaan swasembuh salutan telah dikaji dengan menggunakan mikroskop berkuasa tinggi dan polarisasi potensiometer. Salutan ini juga menunjukkan ketahanan kakisan yang sangat baik dan mencatatkan ciri-ciri filem yang baik.

**Kata kunci:** Swasembuh; penyembuhan UV; salutan alkid; mikrokapsul; minyak kelapa sawit

University of Malaya

## ACKNOWLEDGEMENTS

First of all, grateful and praise be to Allah s.w.t. for the blessing I have been bestowed. I would like to take this opportunity to thank those who are involved directly or indirectly throughout the research. I would like to express my gratitude and utmost appreciation to my supervisor, Dr Desmond Ang Teck Chye for his guidance, support, motivation, patience and opportunity given to me. Special thanks to Professor Gan Seng Neon for taking part to guide me and sharing knowledge for my research. I would like to thank my family especially my mother for continuing support and praying for me. Not to forget my friends and lab mates for their moral support, knowledge and help.

I am also taking this opportunity to thank the staff of Chemistry Department for their help and cooperation. Utmost appreciation to Dr Norshafiza Shahabudin for guiding me in microencapsulation process and Professor Wan Jeffrey Basirun and his team for their generosity and guidance in completing my corrosion study. Finally my appreciation goes to Ministry of Science, Technology and Innovation, Malaysia (MOSTI) (SF-1006) for funding my research.

## TABLE OF CONTENTS

Abstract .....	iii
Abstrak .....	iv
Acknowledgements .....	vi
Table of Contents .....	vii
List of Figures .....	x
List of Tables .....	xii
List of Symbols and Abbreviations .....	xiii
 <b>CHAPTER 1: INTRODUCTION.....</b>	<b>1</b>
1.1 Background of study .....	1
1.2 Problem statement .....	4
1.3 Scopes of research .....	4
1.4 Objectives of research .....	5
 <b>CHAPTER 2: LITERATURE REVIEW .....</b>	<b>6</b>
2.1 Surface coating .....	6
2.1.1 General composition of surface coating .....	8
2.1.2 UV-Curable coating .....	10
2.2 Alkyd resin as binder in coating .....	15
2.2.1 Raw materials .....	16
2.2.2 Synthesis of alkyd .....	21
2.3 Self-healing coating .....	24
2.3.1 Microcapsule for self-healing .....	26



<b>CHAPTER 3: RESEARCH METHODOLOGY .....</b>	<b>29</b>
3.1 Materials.....	29
3.2 Synthesis of palm oil-based alkyd as coating binder.....	30
3.3 Characterization of alkyd .....	31
3.3.1 Determination of total acid number .....	32
3.3.2 Proton nuclear magnetic resonance ( <sup>1</sup> H-NMR) spectroscopy.....	33
3.3.3 Fourier Transform Infrared (FTIR) spectroscopy.....	33
3.4 Microencapsulation of pentaerythritol tetrakis, PETMP and EPON828.....	33
3.4.1 Analysis of microcapsule size and surface morphology .....	37
3.4.2 Core content characterization .....	37
3.4.3 Thermal analysis of microcapsule .....	39
3.5 Preparation of coating mixture .....	39
3.5.1 Treatment of mild steel plate .....	39
3.5.2 Coatings application and curing .....	40
3.5.3 Evaluation of amount of microcapsules loading on self-healing ability..	40
3.5.4 Evaluation of amount of microcapsule on adhesion properties of film on the substrate .....	41
3.6 Analysis of crosslink reaction between EPON828 and PETMP .....	41
3.7 Coating film properties .....	42
3.7.1 Film adhesion tape test.....	42
3.7.2 Water and alkali resistance test.....	44
3.7.3 Acid resistance test .....	44
3.7.4 Salt water resistance test .....	44
3.8 Corrosion study .....	45
3.8.1 Basic corrosion test.....	45
3.8.2 Potentiodynamic polarization test.....	45

<b>CHAPTER 4: RESULTS AND DISCUSSION .....</b>	<b>48</b>
4.1 Synthesis of alkyd .....	48
4.2 Characterization of alkyd .....	48
4.2.1 Acid number .....	48
4.2.2 <sup>1</sup> H-NMR spectroscopy .....	48
4.2.3 FTIR spectroscopy .....	51
4.3 Synthesis of microcapsules .....	53
4.3.1 Surface morphology and size distribution .....	58
4.3.2 Core content analysis .....	61
4.3.3 Thermal analysis of microcapsules .....	66
4.4 Coating mixture preparation.....	71
4.4.1 Evaluation of amount of loading microcapsules on self-healing ability..	71
4.4.2 Effect of amount of microcapsules on adhesion properties of film on the substrate.....	73
4.5 Crosslinked reaction between EPON828 and PETMP .....	74
4.6 Coating film properties .....	78
4.7 Corrosion test .....	79
4.7.1 Basic corrosion tests.....	79
4.7.2 Potentiodynamic polarization experiment .....	81
<b>CHAPTER 5: CONCLUSION AND RECOMMENDATIONS .....</b>	<b>83</b>
5.1 Conclusion.....	83
5.2 Recommendation for Future Study.....	83
References .....	85
List of Publications and Papers Presented .....	90

## LIST OF FIGURES

Figure 2.1: Mechanism for photoinitiators of type I and type II .....	14
Figure 2.2: Structure of polybasic acids that are widely used in alkyd synthesis .....	17
Figure 2.3: Structure of polyols that are widely used in alkyd synthesis .....	18
Figure 2.4: Cross section of oil palm fruit and its oil composition .....	20
Figure 2.5: Reaction scheme of alkyd synthesis .....	24
Figure 2.6: Mechanism of blood clotting .....	25
Figure 2.7: Microcapsule cross-section .....	28
Figure 2.8: Self-healing mechanism using microcapsule approach .....	28
Figure 3.1: Experimental set up of polycondensation process in alkyd synthesis .....	31
Figure 3.2: Summary of microencapsulation of PETMP .....	35
Figure 3.3: Structure of PETMP .....	35
Figure 3.4: Summary of microencapsulation of EPON828 in chlorobenzene .....	36
Figure 3.5: Structure of EPON828 .....	37
Figure 3.6: Coated mild steel attached with electrochemical cell .....	46
Figure 3.7: Set of electrochemical test with three-electrode setup .....	47
Figure 4.1: $^1\text{H}$ -NMR spectra of (a) alkyd, (b) palm olein [Inset shows the structure of alkyd] .....	50
Figure 4.2: FTIR spectra of (a) alkyd, (b) palm olein [Inset shows the structure of alkyd] .....	52
Figure 4.3: Reaction scheme of melamine-formaldehyde .....	55
Figure 4.4: Reaction scheme of urea-formaldehyde .....	57
Figure 4.5: Image of EPON 828 microcapsule observed under a) FESEM, b) digital microscope and c) its size distribution .....	59
Figure 4.6: Image of PETMP microcapsule observed under a) FESEM, b) digital microscope and c) its size distribution .....	59

Figure 4.7: (a) Anatomy of EPON828 microcapsule, (b) image of ruptured EPON 828 microcapsules observed under digital microscope.....	60
Figure 4.8: (a) Anatomy of PETMP microcapsule, (b) image of ruptured PETMP microcapsules observed under digital microscope.....	60
Figure 4.9: (a) Chemical structure of EPON828, (b) $^1\text{H}$ -NMR spectra of neat EPON828 and extracted core of EPON828.....	63
Figure 4.10: FTIR spectra of neat EPON828 and core content EPON828.....	64
Figure 4.11: (a) Chemical structure of PETMP, (b) $^1\text{H}$ -NMR spectra of neat PETMP and extracted core of PETMP.....	65
Figure 4.12: FTIR spectra of neat PETMP and core content of PETMP.....	66
Figure 4.13: (a) DSC thermograms and (b) TGA thermograms; of EPON828 microcapsule, separated core and shell materials.....	68
Figure 4.14: (a) DSC thermograms and (b) TGA thermograms; of PETMP/N,N-dimethylbenzylamine microcapsule, separated core and shell materials.....	70
Figure 4.15: Image of simulated scratch of the coating with 5.0 wt% loaded microcapsules.....	72
Figure 4.16: Image of simulated scratched of self healing coating (a) captured immediately after scratched (b) captured after 3 mins of scratched.....	73
Figure 4.17: FTIR spectra of reaction between EPON828 and PETMP at different time intervals.....	76
Figure 4.18: Assignment peaks of FTIR spectrum of PETMP-EPON828 crosslinked (a) hydroxyl peak, (b) thiols peak, and (c) epoxy peak.....	77
Figure 4.19: Self healed coating (a) before immersed in NaCl solution, (b) after one day immersion in NaCl solution; control alkyd coating (c) before immersed in NaCl solution, and (d) after one day immersion in NaCl solution.....	80
Figure 4.20: Polarization curves of coating samples after 3 hours in contact with 3.5 wt% NaCl.....	82

## LIST OF TABLES

Table 2.1: Differences between free radical and cationic UV curing.....	13
Table 2.2: Properties of alkyd resin based on oil length.....	16
Table 2.3: Composition of fatty acids in palm olein.....	21
Table 2.4: Types of chemical microencapsulation .....	27
Table 3.1: Classification of coating area removal .....	43
Table 4.1: Peak assignments for <sup>1</sup> H-NMR spectra of alkyd and palm olein.....	51
Table 4.2: FTIR assignment peaks for alkyd and palm olein oil.....	53
Table 4.3: The chemical shift of the peaks present in <sup>1</sup> H-NMR spectra of EPON828....	63
Table 4.4: The chemical shift of the peaks present in <sup>1</sup> H-NMR spectra of PETMP .....	65
Table 4.5: Adhesion strength of coating film.....	74
Table 4.6: Physicochemicals properties of coating film .....	79
Table 4.7: Polarization results after immersion in 3.5 wt% NaCl. ....	82

## LIST OF SYMBOLS AND ABBREVIATIONS

$^1\text{H-NMR}$	:	Proton nuclear magnetic resonance
ASTM	:	American Standard Test Method
CPKO	:	Crude palm kernel oil
CPO	:	Crude palm oil
DSC	:	Differential scanning calorimetry
DVB	:	Divinylbenzene
EMA	:	Ethylene maleic anhydride
EPON828	:	Bisphenol A diglycidyl ether
FESEM	:	Field emission scanning electron microscope
FTIR	:	Fourier transform infrared
MF	:	Melamine-formaldehyde
MMA	:	Methyl methacrylate
NACE	:	National Association of Corrosion Engineers
PETMP	:	Pentaerythritol tetrakis (3-mercaptopropionate)
PMF	:	Poly(melamine-formaldehyde)
ROMP	:	Ring opening metathesis polymerization
SH-AS	:	Self-healing after scribe
SH-BS	:	Self-healing before scribe
TGA	:	Thermogravimetric analysis
TMS	:	Tetramethylsilane
UV	:	Ultraviolet
VOC	:	Volatile organic compound
$\delta$	:	Chemical shift

## CHAPTER 1: INTRODUCTION

### 1.1 Background of study

The development of construction and engineering during the period of industrial revolution has spurred the growth of the paint and coating industry worldwide (Miranda, 1993). This is due to the increasing utilization of metal and its alloy in construction such as bridges, buildings and machinery equipment for engineering purposes owing to their high strength and ductility. The continuous exposure of the metals to harsh environment eventually leads to corrosion. This phenomenon will severely affect the economic loss due to function impairment of the metal. Corrosion is a metal degradation as a result from the physicochemical interaction between the metal and its surrounding environment. A study of “International Measures of Prevention, Application and Economics of Corrosion Technology (IMPACT)” conducted by NACE International shows that the global cost of corrosion is estimated to be \$2.5 trillion, which equivalent to 3.4 % of global Gross Domestic Product, GDP (Koch *et al.*, 2016). Application of coating onto the substrate has become one of the popular and versatile methods in corrosion protection besides cathodic protection by sacrificial anode. Coatings are usually applied to metal surface to inhibit corrosion by protecting the substrate from environmental exposure. This coating film prevents the ions from entering the metal surface and thus averts the metal dissolution.

UV-curable alkyd coating is one of the versatile coating that provides film with good physical properties, glossy, durable, easier application and drying tolerance (Gorkum & Bouwman, 2005). UV-curable alkyd coating consists of alkyd which has been used as binder, in which this type of coating renders under UV-radiation to cure in the presence of UV-photoinitiator. Alkyds are mostly derived from vegetable oils since this type of raw material offers an alternative solution to address problems

related to scarcity and high price of the conventional raw material used in surface coating development, petroleum derivatives (Ang *et al.*, 2013; Islam *et al.*, 2014). Palm oil-based alkyd coating shows excellence adhesion properties, and problems related to low hardness can be addressed by introducing unsaturated diacids during alkyd synthesis. D.T.C Ang and S.N. Gan have introduced maleic acid in the synthesis of alkyd derived from palm oil. Maleic acid is a source of C=C that added to increase the amount of unsaturation in the oil. The higher amount of unsaturation in modified palm oil-based alkyd coating increases the ability to cure under UV radiation. According to Ang & Gan, the alkyd in the presence of active diluents is able to UV-cure within short time with better film properties (Ang & Gan, 2012a).

Regardless of all the excellence performance of the coating, the alkyd coating is not an exception when it comes to damages from weathering and from mechanical stress during its prolonged service. External damages are able to be repaired as it can be easily detected. However, the internal damage such as microcracks is undetectable and almost cannot be repaired. When the microcracks are left unattended, it will accelerates the corrosion to take place as the metal surface are now exposed to the oxygen, O<sub>2</sub> and water, H<sub>2</sub>O (Cho *et al.*, 2009). Thus, coating with self-healing material have been extensively studied and exploited. These self-healing materials are inspired by human biological system which is by the process of blood clotting (Ghosh, 2009). Self-healing material is the material with ability to heal by itself.

Self-healing coating may consist of microcapsules, hollow fibres or microvascular systems that are filled with active healing agents. The active healing agents for instances, monomers, dyes, catalyst and hardeners will be released when crack occurs in the coating. In the case that involves microcapsule, when the crack occurs, the microcapsule will rupture and released the active healing agents. The healing agents



will fill the crack and crosslinked upon in contact with catalyst which subsequently solidified. Thus, the crack is said to be self-heal. The crack itself is the driving force for the healing agent to be released by the ruptured of microcapsule.

The most common microcapsule that has been widely used is dicyclopentadiene (DCPD) as healing agent which embedded in polymer matrix. When the crack occurs, microcapsule ruptured and DCPD will flow into crack and react with Grubs' ruthenium catalyst. Polymerization is then starts and the crack is repaired (Brown *et al.*, 2004). S.H. Cho and companions have developed an efficient self-healing system which involved pairs of polydimethylsiloxane/tin catalyst and organic solvents (Cho *et al.*, 2006). Despite of all the excellence self-healing system, they also have some limitation in which heavy metal such as ruthenium and tin are used as they are harmful to environment. Due to carcinogenic and toxicology nature of hexavalent chromates, the use of it has been gradually suspended even though it has been proven to have ability to self-repair (Hamdy *et al.*, 2011; Bhargava & Allen, 2012). Thus, in order to avoid the reliance on toxic material, variety of researches have been developed and exploited towards a greener technology. For example, Suryanarayana and co-worker have developed linseed oil encapsulated in urea-formaldehyde microcapsules as the healing agents. Linseed oil was released from the ruptured capsule and filled the crack. The oil was then dried up upon oxidation to form a film that covers the substrate. Cobalt naphthenate and lead octate was introduced into the coating to speed up the drying process (Suryanarayana *et al.*, 2008). In 2008, Yuan Y.C. and companion have developed pair of epoxy/mercaptan as healant (Yuan *et al.*, 2008). This self-healing system is considered to be more environment-friendly as it does not rely on the usage of heavy metal as the catalyst.

## **1.2 Problem statement**

Typically, coating is applied on a substrate to protect it against corrosion. Regardless of the type of coatings, they are susceptible to damages during its service life time and these damages could vary from formation of apparent macrocracks to almost-invisible microcracks. The latter is usually the result of external damage and it is often visible and can be easily diagnosed. The presence of internal damage such as microcrack however is often undetectable, making it difficult to be repaired. Early detection and repair of microcrack is essential to prevent further fatigue failure of the substrate especially metal surface. It is known that prolong exposure of metal surface towards aggressive environment will eventually accelerates corrosion. One way to address this issue is through the use of self-healing coating, as such coating is able to seal the damages or microcracks when it is formed and prevent further propagation. It is therefore the focus of this project to introduce self-healing property into alkyd surface coating as mean to improve the coating durability and hence, increases the lifespan of the substrate. The self-healing coating model comprised of microcapsules loaded with healing agents, dispersed in alkyd coating matrix. The alkyd coating in this work is formulated as UV curable coating owing to several technical and environmental advantages of such coating over conventional thermal curable coatings.

## **1.3 Scopes of research**

This research focuses on introduction of self-healing ability into UV-curable alkyd coating. Alkyd was synthesized using palm oil as raw material and maleic acid was introduced to increase the amount of its unsaturation in the alkyd to render it UV-curable. Dual-microcapsule system was used to derive self-healing ability in the alkyd coating which consists of a series of EPON828 microcapsule as the healing agent, and microcapsule of pentaerythritol tetrakis (3-mercaptopropionate), PETMP.

#### **1.4 Objectives of research**

The ultimate aim of this work is to produce UV-curable alkyd coating with self-healing ability. To achieve this, the following objectives are spelled out:

- To synthesize palm oil-based alkyd with increased level of unsaturation for UV radiation-curable coating.
- To synthesize EPON 828 and PETMP microcapsules separately and embed both microcapsules into alkyd coatings for self-healing ability.
- To investigate film properties and self-healing ability of alkyd coating formulated with both series of microcapsules.

## CHAPTER 2: LITERATURE REVIEW

### 2.1 Surface coating

Surface coatings have been used as ornamental, protective and functional purposes. Many objects that we encounter in our daily life come in a package with a coating layer. Surface coating is defined as substances that are covering or applied onto the surfaces as a thin continuous layer. Although the terminology between paint and coating often can be used interchangeably, the difference between those two relies on the purposes of each. Paint is defined as pigmented materials which are more properly to called lacquers or varnishes. Generally, most of the paints have been used for aesthetic purposes while surface coating for functional purposes (Marrion, 2004). Those two plays important role in our daily life, even during the early of human civilisation, paint has been used as decorative and functional purpose for instance the murals of The Çatalhöyük. The murals which located at Neolithic site of central Turkey were painted by using pigments that blended with oils (Gündüz, 2016). Despite that, it is a common practice to use coating as a wider term.

Coating can be classified according to their process of application and their drying types. Typically, liquid coating was dried with various methods either physically or chemically such as by evaporative means or curing (cross-linking) by oxidative, thermal or ultraviolet light and other available methods (Ghosh, 2006). The components of coating consist of binder, pigments, additives and solvent. Binder serves as a major component that holds the pigments, filler and additive together to form continuous film. Thus, liquid has been used to disperse the binder to desired viscosity prior for application to the substrate. Liquid used include volatile components (known as solvent-borne coating) and water (known as water-borne coating). These solvents were then evaporated to form dry continuous film. In other words, coating can be classified into solvent-borne paints, water-borne paints and also

powder coating (solvent free). These types of coating form film by physical drying (Lambourne, 1999; Stoye & Freitag, 1998).

Polymer with high molecular mass of binder such as cellulose ester, vinyl resin and chlorinated rubber provide film with good flexibility and stability. This type of binder usually forms film by evaporation of organic solvent as it has low solid content in the mixture. Regardless, this conventional method of drying results in the emission of volatile organic solvent (VOCs). In consideration of human health and environmental issues, solvent based coating has been banned in coating industry. In 1965, coating is one of the major sources of VOC emission behind the gasoline-automobile complex (Jones *et al.*, 2017). Hence, the researches about the water borne-coating and powdered coating have been conducted to replaces this detrimental method (Stoye & Freitag, 1998). The growth of water-borne coating started in early 1865 as the first U.S waterborne paint patent was issued by Flinn and later due to law enforcement such as Clean Air Act Amendment 1990 was strictly imposed (Tiwari *et al.*, 2016). This coating contains higher solids compared to solvent-borne coating. This coating is said to be more environmentally coating compared to solvent-borne coating as it consist only little of solvent used beside water to disperse the film formers for application to the substrate. Thus, resulted in lower emission of VOCs compared to solvent-borne coating.

Nonetheless, film that formed from both coatings (solvent-borne and water-borne coating) relatively sensitive when in contact with solvent, which in turn result in swelling or dissolution. Besides, longer time required to dry or else higher temperature needed to accelerate the drying process. Powder coating involves the heating of powder that adheres to the substrate above its melting point. All the components have been mixed together before being applied to the substrate. Apart from thermosetting,

thermoplastic is mostly used in this coating as binders. Without using solvent, this coating is one of the environmental friendly as there is zero emission of VOCs. Besides that, this type of coating produces film with high durability, resistance towards corrosion and chemicals (Misev & Linde, 1998). Nevertheless, powder coating also has some limitation. Since the process of drying require heating above the temperature of the coating, it is difficult to obtain film with lower  $T_g$  (Ang, 2012).

### **2.1.1 General composition of surface coating**

Coating consists of several components depending on method of application, desired properties, the substrate and ecological and economic constraints. It also comprised as volatile or non-volatile. However, the general components of coating consist of binder, pigment, solvent and additives.

#### **(a) Binder**

Binders are the most important component in the coating as it determines the physical and chemical properties of coating film as well as method of application and drying. Binder, resin, film former or vehicle is the same terms that usually used to describe this film forming component. This components have been used to holds all the ingredients together thus provides the continuous film-forming of the coating. There are two types of binder, which consist of either low molecular weight polymer or high molecular weight polymer. Typically, the higher the molecular weight increases the viscosity of the solution. Low molecular weight polymer needs further chemical reactions to form solid film with high molecular weight. This increasing molecular weight enhanced the physical properties of film (Stoye & Freitag, 1998). The chemical reaction involves either atmospheric oxidation or free radical or condensation of polymerization that induced by radiation (UV, IR, electron beam). Alkyd, polyurethanes, amino resins and phenolic are the examples of binder with low

molecular weight. Nevertheless, binder with high molecular weight polymer may form film physically without further chemical reactions but required to dilute in solvent to suitable concentration for application to form useful film. The examples of binder with high molecular weight polymer are nitrocellulose, solution of vinyl and acrylics, latexes and polyvinyl acetate (PVA) (Lambourne, 1999).

**(b) *Pigment***

Pigments are fine granule solid either organic or inorganic that dispersed in the binder. Pigments are added in the coating to give colours and opacity. The most commonly pigment used is titanium dioxide. While the extenders are coarse inorganic particle that have been used for opacity, although it is not necessarily, it is have been added together with pigment for cost reduction. For example in producing matt white emulsion, a coarse calcium carbonate as extenders that are more cost-effective have been mixed with titanium dioxide to reduce cost. Due to environmental legislation, the conventional inorganic pigments such as lead have been substituted with less toxic coloured pigments (Lambourne, 1999).

**(c) *Solvent***

Solvent is used in the coating to reduce the viscosity of the binder, pigments, filler, extender or additives. It also added to assist in application of coating to the substrate. Thus, the above statements explained the two main purposes of solvent in coating. In some cases, solvent might not act as true solvent for binder but it is actually a true solvent for other components. Thus, diluent is the appropriate term used to describe solvent as it is act as a carrier for binder.

**(d) *Additives***

Additives are added in the coating in small amount to improve specific properties of coating. Additives usually were named according to their mechanism (Stoye &

Freitag, 1998). Usually the coating either liquid or dry films might encounter deficiencies in their properties without the presence of additives. The deficiencies might include settlement of pigment and skinning; aeration and bubble retention on application; cissing, sagging and shrivelling on the film (Lambourne, 1999). Antisettling agents can be added to overcome the settlement and skinning problem of coating. The aeration and pore on application might reduce by adding film-formation promoters for example high boiling points ethers and glycol ether ester which often combined with hydrocarbon (Stoye & Freitag, 1998).

### **2.1.2 UV-Curable coating**

Apart from those coatings mentioned in section 2.1 that have been developed for replacing solvent-borne coating. This technology has been developed for industrial application in 1970s. Due to the enforcement of legislation such as Clean Air Act Amendment 1990 worldwide, the research towards more environmental friendly coating has actively being studied (Weiss, 1997). UV-curable coating is preferable over thermal radiation coating in coating drying method to minimize the emission of harmful volatile organic compounds (VOCs). This is due to the heavy usage of organic solvents in thermal radiation coating (Sørensen *et al.*, 2009). Such problem is not relevant in UV-radiation curable coating because such coating uses reactive diluents instead of the usual organic solvents. In this type of coating, UV radiation activates the light sensitive component (photoinitiator) that added in the coating formulation. This photoinitiator will then initiate the polymerization. Since the mechanism of drying involves the polymerization of reactive components in the formulation, there is no volatile solvent have been used. Reactive components may be obtained from higher molecular weight of oligomers (binder) and lower molecular weight monomers (usually reactive diluent). The entire components stay within the film upon drying, thus no emission of VOCs occur (Glöckner *et al.*, 2008).



In the coating mixture, the reactive diluents were added to dilute the oligomers to suitable viscosity for coating application. It also took part in the crosslinking of coating resin to form homogenous film (Ali *et al.*, 1994). However, the selectivity of reactive diluent plays an important role in contribution to the film properties. In a study conducted by D.T.C. Ang reveals that alkyd coating with divinylbenzene, DVB as reactive diluents is suitable for use in high-temperature applications and provides better protection to the substrate due to its bifunctional. Nonetheless, its bifunctionality resulted in poor adhesion strength of the film due to rapid development of internal stress. Alkyd coating with methyl methacrylate, MMA show excellence adhesion performance due to high polarity that improve the interfacial interaction between coating and the substrate (Ang, 2015).

Other advantage of UV-curable coating includes fast drying speed. Dry film can be obtained just within a few minutes and thus resulted in higher production rate. Besides that, UV curable coating is known to provide films with excellence performance such as high durability and toughness; and high mechanical and chemical resistance owing to high crosslink density during curing (Ang *et al.*, 2013; Schwalm, 2007). Besides that, this type of radiation curing produces films with excellent physicochemical properties and also has higher production rate owing to short curing time (Ang & Gan, 2012b).

#### (a) ***Components in UV-curable coating***

General components of this coating consist of binder, reactive diluents, photoinitiators and additives. In this coating, oligomers act as a binder which provide reactive site for polymerization. This component is a major component that covers the formulation typically ranging from 50-80 %. Since no solvent used to reduce the viscosity of the formulation, usually low molecular weight of oligomers are used to

ensure low viscosity of formulation (Glöckner *et al*, 2008). The types of oligomers used also determined the properties of the coating film as a whole (Ang, 2012).

The source of monomer can be found in reactive diluent which consist of compound with low molecular weight. This diluent was added not only for reactive site for polymerization but also to reduce viscosity of oligomers for application. Thus, it is suitable as substitution of solvent used in conventional coating as low or almost no emission of VOCs. These two components involve in the polymerization during curing process which later forming film.

Photoinitiator plays important role in this coating as it initiate the polymerization and control the speed of curing. The photoinitiator must be able to absorb light and thus undergo photolysis. Polymerization of the reactive components can be initiated by two types of photoinitiator which involves free radical and cationic. Table 2.1 shows the differences between two types of photoinitiator.

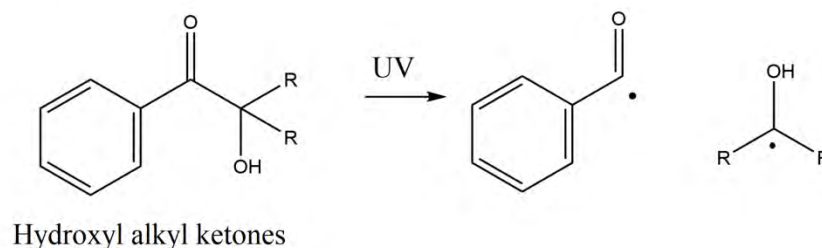
**Table 2.1:** Differences between free radical and cationic UV curing

<b>Free radical UV curing</b>	<b>Features</b>	<b>Cationic UV curing</b>
Acrylates, unsaturated polyester/ styrene resins	<b>Binder</b>	Epoxies and vinyl ether
Produces free radical	<b>UV exposure and initiation</b>	Produces protons or Lewis acid
Free radical recombine with the oligomers results in consumption of radicals	<b>Mechanism</b> <b>-Propagation</b>	Continuous propagation of cations results in consumption of oligomers.
A few seconds	<b>Rapidity of curing</b>	Seconds to minutes
-Oxygen inhibition	<b>Surrounding inhibition</b>	-Not sensitive to oxygen
-Not sensitive to moisture		-Moisture and bases inhibition
Shrinkage of acrylates during polymerization	<b>Shrinkage</b>	Lower shrinkage due to the ring-opening polymerization step
Good	<b>Adhesion on substrate</b>	Excellent

(Adopted from P. Glöckner et al (2008). *Radiation curing coatings and printing inks*. Hannover: Vincentz Network)

In general, radical photoinitiators comprised of two classes which type I and type II. Type I photoinitiator involve unimolecular cleavage while type II undergo bimolecular reaction which involves hydrogen abstraction of co-initiator by excited state of photoinitiators to form radicals. Figure 2.1 shows the photoinitiators mechanism of different classes of photoinitiators.

### Type I photoinitiator



### Type II photoinitiator

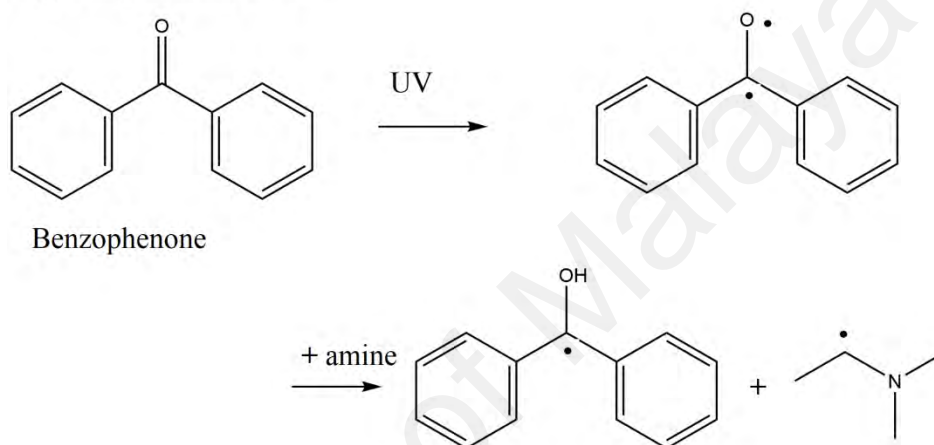


**Figure 2.1:** Mechanism for photoinitiators of type I and type II

(Adopted from P. Glöckner *et al* (2008). *Radiation curing coatings and printing inks*. Hannover: Vincentz Network)

#### (b) *Free radical polymerization during UV curing*

The general mechanism involves initiation, propagation and chain termination step. In the initiation step, the photoinitiator was activated by absorbing UV radiation. The two classes of photoinitiator which are type I and type II were initiated by the mechanism mentioned in previous section. The propagation step proceeds with the addition of monomer to a radical chain. The rate of propagation relies on initiation rate and oligomer reactivity (Glöckner *et al*, 2008). The free radicals are produced continuously at every step and react rapidly, thus increased the rate of propagation (Ang, 2012). At termination steps, the radicals are combined forming one molecule of long chain.

## 2.2 Alkyd resin as binder in coating

Alkyd is one of the predominant binders in coating industry since early 1930's. The terminology of alkyd originated from the words polyhydric alcohol 'al' and polybasic acid 'cyd' which latter altered to 'kyd'. Kienle introduced the term alkyd in 1927 to describe the end product of reaction between alcohol and acid (Heitkamp & Pellowe, 1995). Basically, alkyd is polyester that derived from the reaction between triglyceride of vegetable oils, polyols and dibasic acid or their anhydride. Due to its excellence mechanical properties, easily modified into desired film and drying method, easy application and economical, it have been widely used in paint and coating industry as binder. The invention of alkyd was started by Berzelius in 1847 when he produced intermediates of alkyd by reaction of glycerol with tartaric acid, followed by Betherlot in 1853. In 1901, Smith has developed brittle polyester by the reaction of glycerol with phthalic anhydride. The investigation between polyhydric alcohols and polybasic acid has continued since then when Carothers discovered the flexibility and curing properties of this polymer. In 1920 Kienle from General Electric Company modified the alkyd derived from vegetables oil and fish oil. This oil-modified alkyd improved the film properties which suitable for binder (McIntyre, 2003; Lanson, 1985). The exploration of alkyd continued with investigation conducted by General Electric Company and starting in year 1930, the production alkyd has dominated the coating industry.

Alkyd can be classified into short oil, medium oil and long oil. These oil lengths were determined by the weight percent of fatty acid. The increasing oil content contributes the alkyd with the properties close to the oil for instances increasing ability in oxidation drying, solubility in aliphatic hydrocarbons and flexibility. Conversely, the shorter the oil length, the more alkyd resemble the polyester chains properties (Gündüz, 2016). The properties of the alkyd such as drying time, flexibility,

mechanical and chemical resistance of film are related to the oil content or the type of fatty acid (Heitkamp & Pellowe, 1995). Table 2.2 shows the properties of alkyd resin related to oil length. Generally, the oil with fatty acid content <45% are classified as short oil alkyd while (45-55) % as medium oil alkyd and >55% as long oil alkyd (Gündüz, 2016).

**Table 2.2:** Properties of alkyd resin based on oil length

<b>Features</b>	<b>Short oil</b>	<b>Medium oil</b>	<b>Long oil</b>
<b>Solvent</b>	Most polar	Intermediate	Less polar
<b>Compatibility with others binder</b>	Most compatible	Intermediate	Less compatible
<b>Viscosity</b>	Higher viscosity	Intermediate	Less viscous
<b>Brushability</b>	Less brushability	Intermediate	Higher brushability
<b>Dry</b>	Through dry	Through dry	Through dry
<b>Outdoor durability</b>	Outdoor durability	Outdoor durability	Outdoor durability
<b>Hardness</b>	Higher	Intermediate	Lower

(Adopted from Manea, M. (2008). *High Solid Binders*. Hannover: Vincents Network GmbH)

### 2.2.1 Raw materials

#### (a) *Polybasic acid*

Polybasic acid is an acid that have more than one replaceable hydrogen atoms. Polybasic acid with aromatic ring is the most widely used in alkyd formulation due to the rigidity of aromatic ring increases the  $T_g$  of the resin (Jones *et al*, 2017). Phthalic anhydride had been preferably used due to the ability to react at low temperature prior to the low melting point (131 °C) compared to other dibasic acid. The esterification reaction temperature is in the range of (230 - 250) °C. Besides that, it will improve

solubility, hardness and chemical resistance of alkyd resin (Isaac & Nsi, 2013). The anhydride used also reduced the water produced as by product, thus the water removal during polyesterification can be reduced (Gündüz, 2016). Other polybasic acid that has been used include isophthalic acid, terephthalic acid, glutaric anhydride, maleic anhydride and succinic anhydride.

Isophthalic acid produces alkyd with more tougher, faster drying and high chemical resistance. The reaction with isophthalic acid form intramolecular cyclic ester by meta position of carboxylic group which eventually increase the molecular weights and viscosities of alkyd (Holmberg, 2001). Despite that, the high melting point of isophthalic acid (330 °C) exceeds the reaction temperature of esterification process. As a result, the production of alkyd required longer reaction time and higher temperature in the esterification process, thus increases the cost of alkyd production as a whole (Isaac & Nsi, 2013). Maleic anhydride was also being introduced in alkyd formulation to improve colour and water resistance (Holmberg, 2006). Maleic anhydride was added in the formulation in small amount and reacts with polyol. The introduction of maleic anhydride increases the double bond in alkyds (Gündüz, 2016). Figure 2.2 shows the most common of polybasic used in alkyd formulation.

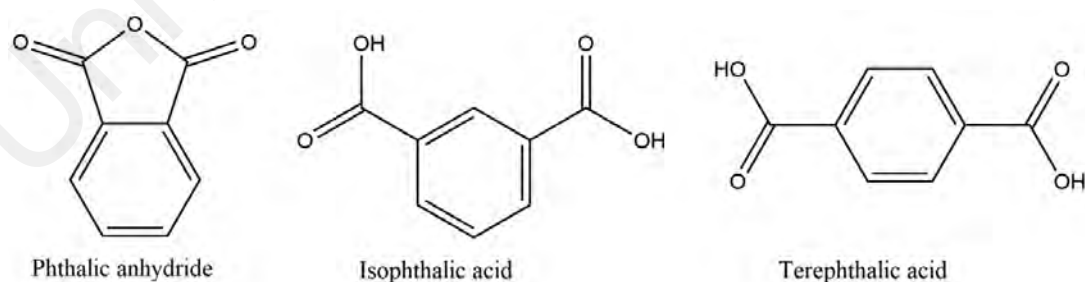


**Figure 2.2:** Structure of polybasic acids that are widely used in alkyd synthesis

(b) **Polyols**

The selection of polyols in alkyd formulation is important for the degree of branching of the alkyd. The most commonly polyol used is glycerol and pentaerythritol. Glycerol that consists of three hydroxyl group is the most common used with long oil and short oils of alkyd. It can be dissolved in many solvents, and produced excellent thin film (Gündüz, 2016).

Pentaerythritol, PE contains four hydroxyl groups. The tetrafunctionality of pentaerythritol increases the possibility to form gelation although the alkyd produced has faster drying ability, improved hardness and glossy. This is due to higher branching formation which makes it difficult to control the reaction. Thus, the formulations of alkyd with PE as polyols is suitable to be used with long oils but limited to short and mediums oils (Gündüz, 2016).

Trimethylolpropane has slower rate of esterification and the produced alkyd have narrowed molecular weight distribution and lower viscosity compared to alkyd formulation with glycerol. The primary hydroxyl group is sterically hindered by the neopentyl structure (Jones *et al*, 2017). Figure 2.3 shows the most common polyols used.

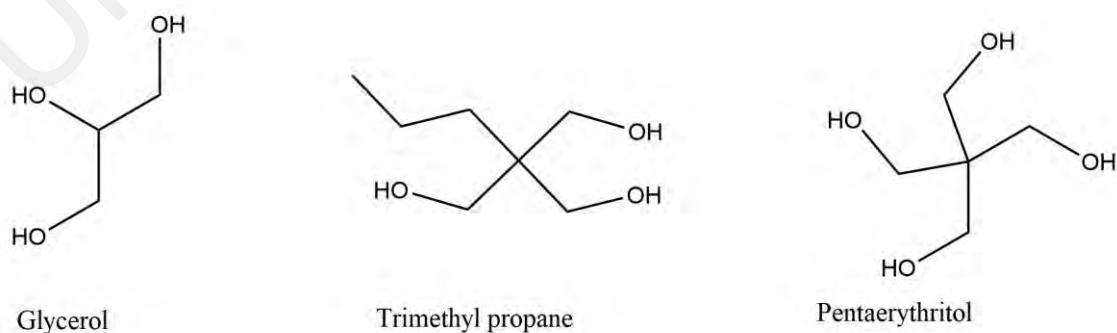


**Figure 2.3:** Structure of polyols that are widely used in alkyd synthesis



### (c) *Palm oil and fatty acids*

The properties of alkyd are mainly controlled by oil selection. Vegetables oil that has been used as raw material of binder can be classified into drying oils, semi-drying oils and non-drying oils. This classification is determined by their iodine value. Alkyd can also be classified as oxidizing and non-oxidizing alkyd. The oxidizing alkyd consists of drying or semi-drying (unsaturated) oils in which the drying process involves the oxidation of polyene structures in excess fatty acid (Gündüz, 2016; Holmberg, 2006). The examples of drying oils include linseed, soybean, tung, sunflower and dehydrated castor oil. These oils are known to have good drying ability. On the other hand, the non-oxidizing alkyd involves non-drying (saturated) oils which have poor drying abilities. The drying process of this non-oxidizing alkyds is by curing as it is not be able to undergo oxidation due to lack of unsaturation of fatty acid (Holmberg, 2006). The sources of non-drying oil include palm oil and coconut oil.

Palm oil is one of the edible vegetable oils that obtained from the extraction of mesocarp of the oil palm fruit. Oil palm tree or scientifically called *Elaeis guineensis* is originated from West Africa oil palm and has been brought to Malaysia in 1870s by British (Teoh, 2002). Malaysia has become world's second largest producer of palm oil as Indonesia has surpassed Malaysia in 2006 for oil production (Bentivoglio *et al.*, 2018). Generally, there are two products of oil that can be obtained from the kernel and mesocarp of palm fruit. The oil that obtained from kernel which is fruit seed is known as crude palm kernel oil (CPKO) while crude palm oil (CPO) obtained from the mesocarp which is the flesh of oil palm fruit. The composition of saturated fatty acid of palm oil is almost equal to composition of unsaturated fatty acid which eventually makes the palm oil as non-drying oil. The unsaturated fatty acid consists of 40% oleic acid (monounsaturated fatty acid) and 10 % linoleic acid (polyunsaturated

fatty acid) while saturated fatty acid consist of 45 % palmitic acid and 5 % stearic acid (Barcelos *et al.*, 2015).

Palm olein is a liquid component at ambient temperature (generally at warm climate) that is obtained from crude palm oil. Crude palm oil that semi-solid at room temperature (20 °C) undergo physical fractionation. The fractionation separated the palm oil into liquid and solid component. The liquid component is known as palm olein while solid component as palm stearin. Figure 2.4 shows the fruit palm cross section and palm oil composition. Palm olein has high stability against oxidation and easily blended with other oils. The composition of fatty acid in palm olein is almost equal to the composition in palm oil. The saturated fatty acid in palm olein, palm oil and also palm stearin has more than 47 % of the total fatty acid (Tan & Nehdi, 2012). Table 2.3 shows the fatty acid composition in palm olein.

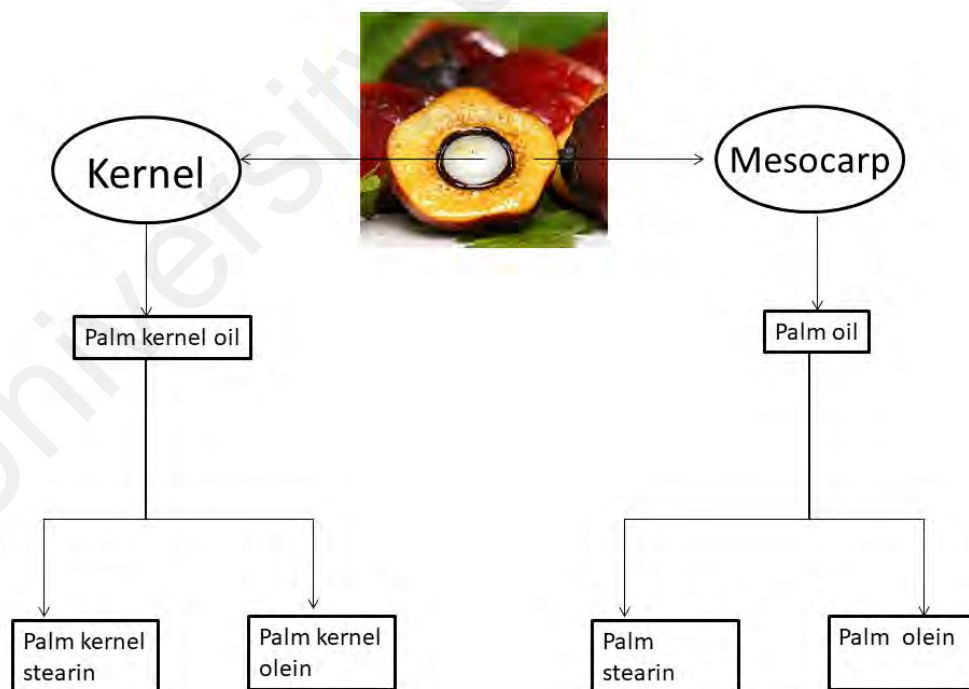


**Figure 2.4:** Cross section of oil palm fruit and its oil composition

**Table 2.3:** Composition of fatty acids in palm olein

Fatty acid	Fatty acid chain length	Mean
Myristic	C 14:0	1.0
Palmitic	C 16:0	39.8
Stearic	C 18:0	4.4
Oleic	C 18:1	42.5
Linoleic	C 18:2	11.2
Linolenic	C 18:3	0.4

(Source: Malaysian palm oil industry (2011). Retrieved 26, August, 2018 from [http://www.palmoilworld.org/about\\_malaysian-industry.html](http://www.palmoilworld.org/about_malaysian-industry.html))

### 2.2.2 Synthesis of alkyd

The alkyds syntheses can be done by two process which either from monoglyceride process or fatty acid process. In monoglyceride process, the triglyceride oil was used in the reaction with polyol and polybasic acid. However, this process produces a heterogeneous mixture of triglyceride and unmodified polyester as polyol tend to react with acid. Thus, to overcome this problem, this process was modified into two steps which consist of alcoholysis of oils and polycondensation of monoglycerides. In alcoholysis step, triglyceride of oil is pre-reacted with polyol into a reactive monoglycerides. Triglyceride oil was heated with glycerol prior to alcoholysis reaction temperature in the presence of basic catalyst. The catalyst such as calcium hydroxide,  $\text{Ca(OH)}_2$ , lead oxide, PbO and Ca-soaps was added in this step to increase the reaction rate of ester. The reaction continued until monoglycerides are obtained. The second step was then continued by condensation of monoglycerides and polyacids, thus producing alkyd with desired viscosity or acid value.

In the fatty acid process, fatty acid has been used instead of triglyceride oil. This process was carried out in a single step by adding fatty acid to the reaction of polyol and diacid. Thus, this single step reduced the process time owing to the presence of carboxylic group in the fatty acid, which the polyol preferentially to react with. Besides that, this process can be controlled easily in terms of polyol selection, molecular weight of resin and the acid value during condensation. Lower acid value can also be obtained in this process which later contributes to drying properties of the alkyd. Nonetheless, this process required an expensive cost as the fatty acid need to be separating from the mixtures in a first place. Thus, as an alternative the fatty acid used usually mixed with the oils in this process to reduce cost (Holmberg, 2006; Gündüz, 2016).

Islam and companion have synthesized palm oil based alkyd by using monoglyceride method in which this method consist of two step of process. Phthalic anhydride and maleic anhydrides have been added as polybasic acid during the second step which is transesterification (Islam *et al.*, 2014). Phthalic anhydride which commonly used in alkyd synthesis is insoluble in oil but soluble in glycerol. Thus, to avoid the formation of glyceryl phthalate gel particles during the initial process, the alcoholysis of oil with glycerol was carried out at separate step (Wicks, 2002).

Maleic anhydride was introduced to increase the amount of unsaturation into the main chains of alkyd (Ang & Gan, 2012b). This is due to the difficulty in drying due to the non-drying properties of palm oil in the palm oil based alkyd (Islam *et al.*, 2014). The low iodine value of palm oil compared to other oil, which translates to lower degree of unsaturation (Islam *et al.*, 2014). Unmodified alkyd coating produced from such oil tend to exhibit lower hardness and impact strength compared to that from soybean oil (Issam & Cheun, 2009). This study was supported by F.S. Guner *et*

al in which most of the alkyd was synthesized using drying oil such as sunflower oil, soybean oil and linseed oil (Guner *et al.*, 2006; Ang, 2012). Different ratios of phthalic anhydride and maleic anhydride produced different properties of alkyd in terms of glossy, thermal stability and physical and chemical resistivity (Islam *et al.*, 2014). This study was also supported by Chiplunkar and Pratap in the investigation of synthesis of alkyd resin from sunflower acid oil. The increase value of maleic anhydride improved the drying and film properties of the alkyd resins which in turn may be suitable to be used as a binder in surface coating (Chiplunkar & Pratap, 2016). Figure 2.5 shows the reaction scheme of alkyd synthesis.

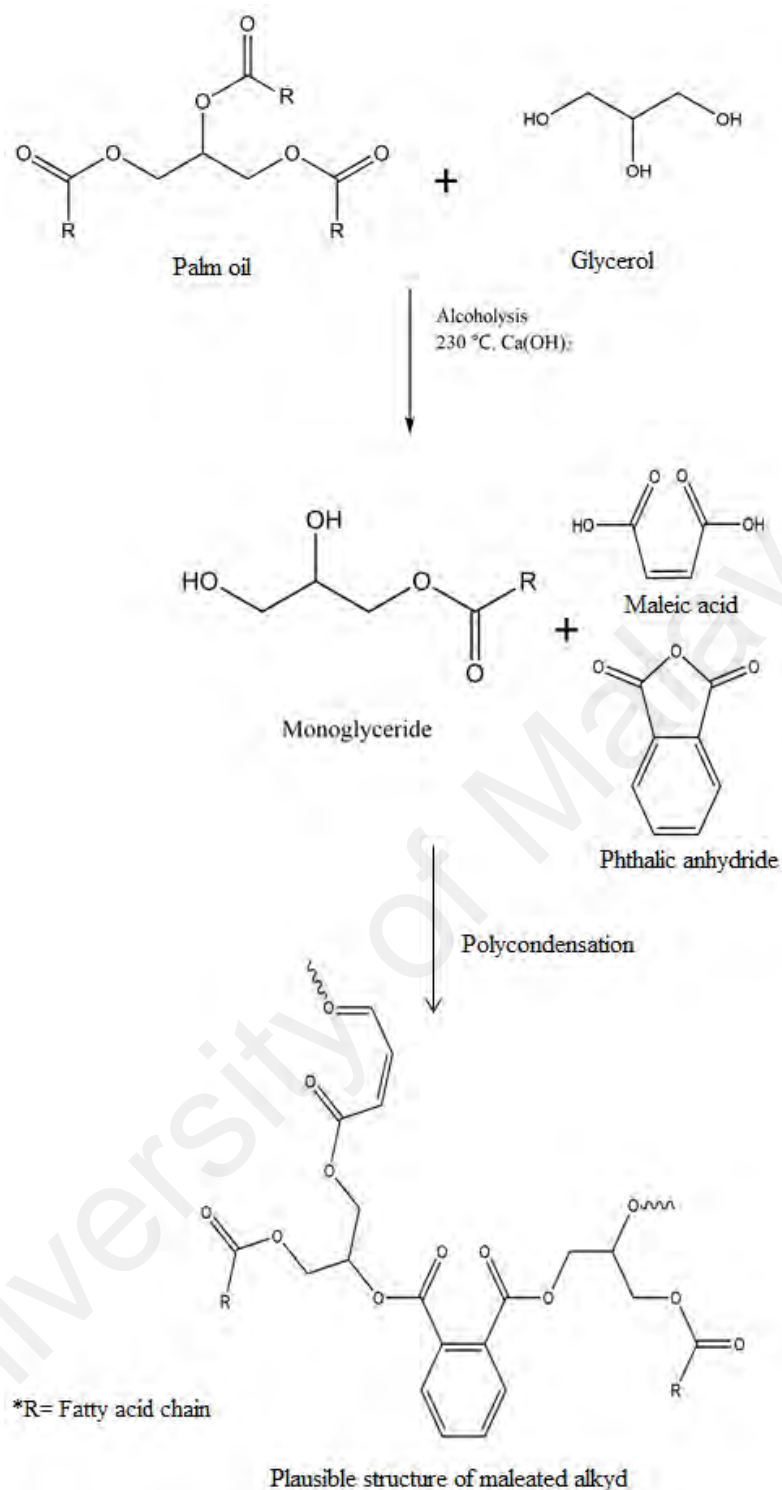


**Figure 2.5:** Reaction scheme of alkyd synthesis

### 2.3 Self-healing coating

Advanced technology has developed self-healing material that inspired by human biological system such as the process of blood clotting. In the process of blood

clotting, when an injury or cut occur at the surface of the skin, human biological system immediately stop the bleeding by activating the platelets and lump at the wound site to heal. The platelets release the clotting factors and seal the wound. Thus, it inhibits the introduction of foreign matter and regrows the epidermis cell. Figure 2.6 shows the mechanism of blood clotting process. This interesting self-defense mechanism of human system has inspired the researchers to mimic and develop synthetic self-healing polymer materials. Self-healing material is a material that has ability to heal by itself. All the materials that exist especially its material coating are not exception when encounter wears during its service. The formation of internal damage such as microcracks is difficult and almost impossible to be detected. This situation will eventually lead to corrosion when exposed to environment as the damage is left unattended. Thus, self-healing material has been a major breakthrough in coating industry to delay further failure and malfunction of the materials by protecting it from corrosion.

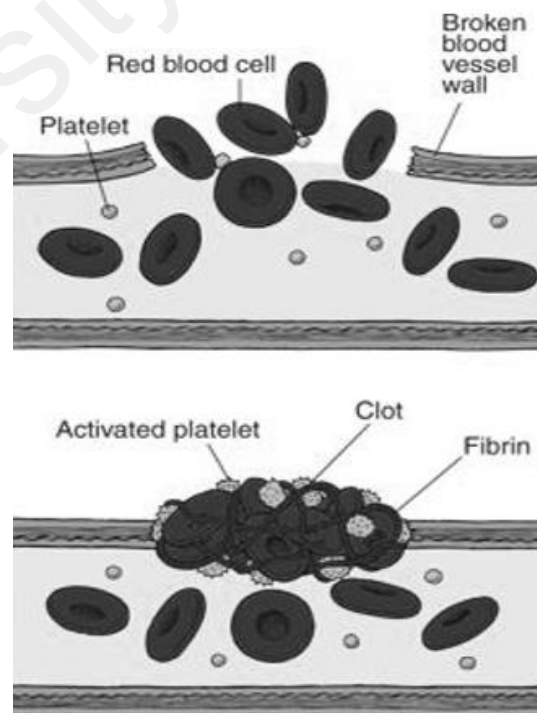


**Figure 2.6:** Mechanism of blood clotting

(Source: Moake, J.L. (2017). *Merck manuals consumer version*. Merck & Co. Inc)

Self-healing material may involve autonomous and non-autonomous. Autonomous self-healing material is spontaneous self-repair without external force whereas non-autonomous self-healing materials need external force or stimuli to initiate the healing process, for instances thermal, radiation, pH changes, pressure changes and mechanical action (Stankiewicz *et al.*, 2013). The most common approaches in self-healing system are by the embedment of micro/nanocapsules, embedment of hollow fibres and microvascular system into the polymer matrix (Samadzadeh *et al.*, 2010). These three systems consist of liquid healing agents containing such as monomers, dyes, catalyst and hardeners. The mechanism of self-healing begins with the proliferation of crack which eventually cause these reservoirs to ruptured and release healing agents to the damage site. The crack was then healed upon solidified and thus protected against harsh environment. In 1996, Dry discovers the potential of self-healing polymeric system that involves hollow fibres to repair the internal cracks. This hollow fibre consists of healing agents that eventually released and seal the damage site (Dry, 1996). White *et al* later designed the self-healing system with microcapsule approach in 2001. Dicyclopentadiene (DCPD) was used as monomer was encapsulated and embedded in polymer matrix (White *et al*, 2001).

### **2.3.1 Microcapsule for self-healing**

Microcapsule in self-healing system is the approach that is most studied due to easily embedded and distributed uniformly of microcapsule in the polymer matrix (Samadzadeh *et al.*, 2010). Besides that, this approach minimizes the difficulty during manufacturing period compared to difficulty face by hollow fibre approach (Aïssa *et al.*, 2012). In general, microcapsule involves healing agents as core content and polymeric shell material. The polymeric shell material used must be inert to chemical healing agent. Microcapsule can be encapsulated by either chemically or physically. Chemical microencapsulation involves suspension, emulsion, in situ polymerization



and interfacial polymerization while physical microencapsulation involves coacervation and sol-gel encapsulation (Giro-Paloma *et al.*, 2015). Table 2.7 shows the advantages and disadvantages of chemical processes of microencapsulation.

**Table 2.4:** Types of chemical microencapsulation

Techniques	Mechanism	Advantages	Disadvantages
Suspension polymerization	Monomer was added to the liquid phase	Good heat control of the reaction  Cost effective	Few monomers are water soluble.  Size around 2-4000 $\mu\text{m}$
Emulsion polymerization	Monomer was added in a continuous phase of water and emulsified (with added surfactant)	High molecular weight polymer  Fast	-
In situ polymerization	Direct polymerization by single monomer on particle surface.	Uniform cost	Purify polymer from the surfactant  Size between 1 and 2000 $\mu\text{m}$
Interfacial polymerization	The capsule shell formed at or on the surface of the droplet or particle by polymerization of the reactive monomers.	Versatile, good properties in size, degradability, mechanical resistance	Size 2- 2000 $\mu\text{m}$

(Adopted from Giro-Paloma, J., Martínez, M., Cabeza, L. F., & Fernández, A. I. (2016). Types, methods, techniques, and applications for microencapsulated phase change materials (MPCM): A review. *Renewable and Sustainable Energy Reviews*, 53, 1059-1075.)

Figure 2.7 shows the cross section of microcapsule. Figure 2.8 shows the mechanism of self-healing by microcapsules. This self-healing coating includes EPON828 and PETMP microcapsule embedded in the alkyd coating matrix. When the crack occurs, the propagation of crack ruptures the embedded microcapsules and releases the healing agents (EPON828 and PETMP). The healing agents fill the crack plane and activated to react with one another when in contact with catalyst (N,N-dimethylbenzylamine). The healing agents crosslinked and solidified forming a protective layer that covers the crack site, inhibit the substrate being exposed to environment. This healing model is another variation to the one developed by White *et al* which utilized the ring opening metathesis polymerization (ROMP) of dicyclopentadiene, DCPD in the presence of ruthenium (Ru) based Grubbs' catalyst in their model. Both DCPD and catalyst were encapsulated and embedded in the polymer matrix (White *et al*, 2001).

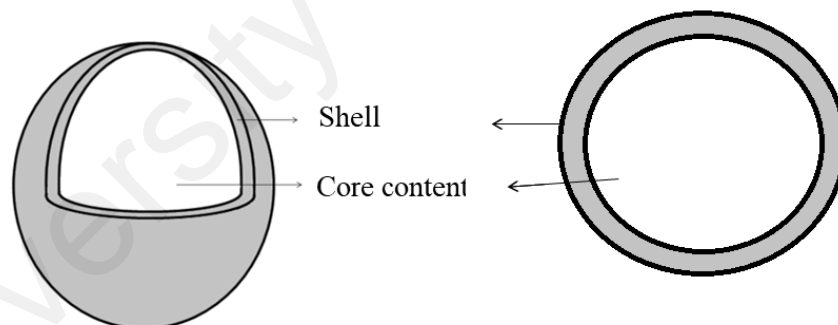


**Figure 2.7:** Microcapsule cross-section

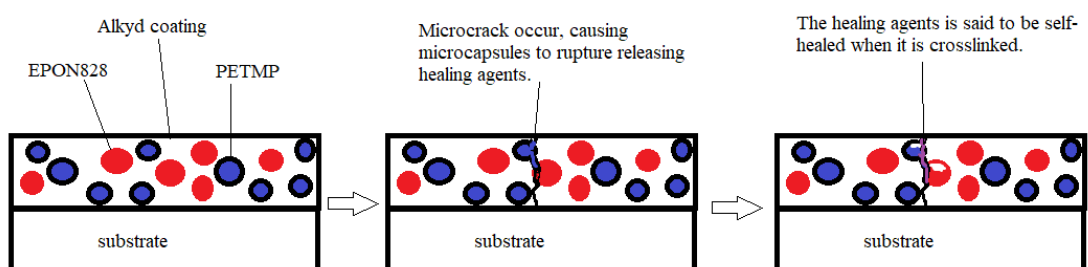


**Figure 2.8:** Self-healing mechanism using microcapsule approach

## CHAPTER 3: RESEARCH METHODOLOGY

### 3.1 Materials

Chemicals for coating mixture, methyl methacrylate (MMA),  $\geq 99\%$  was obtained from Friendemann Schmidt Chemical (Parkwood, Western Australia) and benzophenone 99% was obtained from Sigma Aldrich (Steinheim, Germany).

Alkyd as coating substrate was synthesized by using refined olein palm oil obtained from Sime Darby (Malaysia) while glycerol with 99.5% purity was obtained from Friendemann Schmidt (Parkwood, Western Australia). Phthalic anhydride ( $C_8H_4O_3$ ) with purity  $>98\%$  was obtained from R&M Chemicals (Selangor, Malaysia) and maleic acid ( $C_4H_4O_4$ ) with purity  $\geq 99\%$  was obtained from Merck (Darmstadt, Germany). Calcium hydroxide, 95% which used as catalyst was obtained from HmbG Chemicals.

For synthesis of EPON 828 microcapsule, bisphenol A diglycidyl ether (EPON828) used as epoxy core material was obtained from ASA CHEM (Selangor, Malaysia). Shell forming material, urea ( $NH_2CONH_2$ ) (5M in  $H_2O$ ) and ammonium chloride ( $NH_4Cl$ ), with purity 99.99% was purchased from Sigma Aldrich (Darmstadt, Germany). Formaldehyde 37% and, chlorobenzene, 99.5% were obtained from RCI Labscan (Bangkok, Thailand) while resorcinol,  $\geq 99.0\%$  and ethylene-maleic anhydride copolymer (EMA) was provided by Sigma Aldrich (St. Louis, USA).

For microencapsulation of hardener, pentaerythritol tetrakis (3 – mercaptopropionate), PETMP with purity  $\geq 95\%$  for core material was obtained from Sigma Aldrich (USA). The microcapsule shell wall forming material, 2,4,6-triamino-1,3,5-triazine (melamine),  $\geq 99\%$  and 37 % formaldehyde from Merck (China) and RCI Labscan (Bangkok, Thailand), respectively. Aqueous solution sodium styrene maleate copolymer (13 wt% in  $H_2O$ ) obtained from Sigma Aldrich (St. Louis, USA),

whereas citric acid, 99.5-100.5% and triethanolamine,  $\geq 99\%$  as pH regulator were obtained from Merck (Austria) and (Darmstadt, Germany), respectively. N,N-dimethylbenzylamine,  $\geq 99\%$  was obtained from Sigma Aldrich (Germany).

### **3.2 Synthesis of palm oil-based alkyd as coating binder**

Refined palm olein has been used in synthesis of alkyd as it provides the source of fatty acid. There are two processes involved in the synthesis of alkyd in which included alcoholysis and esterification. This method was adopted from the method employed by Ang and Gan. (Ang & Gan, 2012a). The produced alkyd was then characterized accordingly.

Synthesis of alkyd involves two step reactions which is alcoholysis of palm olein and glycerol, followed by polycondensation of monoglyceride in the presence of acid anhydride. 304.5 g of palm olein oil, 166.9 g of glycerol and 0.2 g of calcium hydroxide,  $\text{Ca}(\text{OH})_2$  catalyst were added into a reaction flask. The reaction flask was equipped with a reflux condenser, digital thermometer and mechanical agitator. Liebig condenser was attached to the reaction flask to avoid volatile substances leaving the system and also to avoid development of high pressure in the flask. The alcoholysis process began with heating the mixture up to  $230\text{ }^\circ\text{C}$  with constant stirring at 250 rpm for 2 hours. The temperature of the reaction was remaining constant for 2 hours. After 2 hours reaction, the temperature of the reaction mixture was then lowered to  $<150\text{ }^\circ\text{C}$  as the heating was turned off.

Monoglycerides formed from the alcoholysis process was then allowed to undergo polycondensation with 179.2 g of phthalic anhydride and 60.2 g of maleic acid at  $220\text{ }^\circ\text{C}$ . The temperature during polycondensation is held constant. Throughout the polycondensation process, the reaction flask was equipped with Dean-stark decanter attached to a condenser, as shown in Figure 3.1. Dean-stark decanter serves to collect

the water, a by product of condensation of diacids and glycerides. Since this reaction is reversible, it is important to ensure that the by product was removed from the system to reduce the occurrence of reversed reaction where ester linkages are hydrolysed

(Ang, 2012). The extent of polycondensation was monitored by performing periodic total acid number test (ASTM D1639-90). The reaction was allowed to continue until the acid number of the mixture dropped to below 10% from initial. Throughout the reaction, vigorous agitation needed to ensure the consistency of the final product (Heitkamp & Pellowe, 1995).

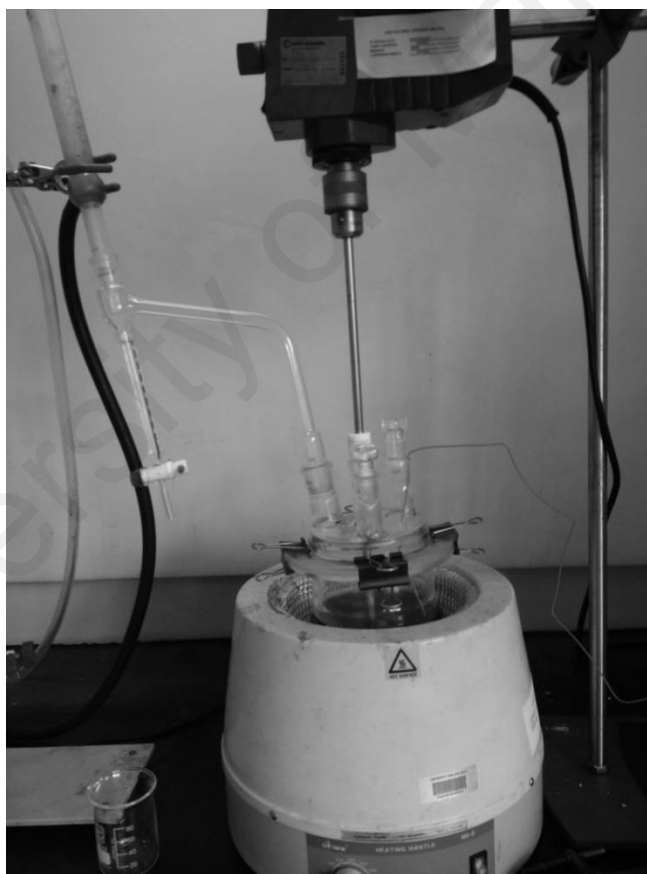


**Figure 3.1:** Experimental set up of polycondensation process in alkyd synthesis

### **3.3 Characterization of alkyd**

The alkyd produced was characterized by determining its acid number to determine the amount of free carboxylic acid. Structural analysis of alkyd was identified by

Fourier transform infrared spectroscopy (FTIR) and nuclear magnetic resonance spectroscopy (NMR).

### 3.3.1 Determination of total acid number

The acid number in alkyd was determined by performing periodic total acid number test that follow ASTM D1639-90. Total acid number was measured by the amount of potassium hydroxide (KOH) needed in milligram to neutralize the free fatty acids in one gram alkyd. Prior to titration with alkyd, potassium hydrogen phthalate (KHP) was used to standardize the concentration of KOH. 1 g of KHP was dissolved in 20 ml distilled water and phenolphthalein indicator was added. Meanwhile, KOH was dissolved in 1L methanol. KHP solution was then titrated against KOH solution until the first appearance of permanent pale pink colour.

The total acid number test was performed on alkyd sample periodically (every 1 hour interval) during alkyd synthesis 1g of alkyd was dissolved in neutral solvent consist of the mixture of isopropanol and toluene (1:1) with phenolphthalein as indicator. The sample mixture was titrated against KOH solution until the first appearance of permanent pale pink colour. The acid number, A of the alkyd can be calculated by using the following formula:

$$A = VK / SN \quad \text{Equation 3.1}$$

Where:

V = Volume of KOH (mL) solution used in titration

K = Concentration of KOH solution (mg/mL) for sample titration

S = Weight of sample (alkyd)

N = Normality of KOH

### 3.3.2 Proton nuclear magnetic resonance ( $^1\text{H}$ -NMR) spectroscopy

$^1\text{H}$ -NMR analysis on alkyd was also conducted to obtain its chemical structure. The alkyd was dissolved in deuterated chloroform containing 99.8%  $\text{CDCl}_3$  and 0.03% of tetramethylsilane (TMS). The sample was analyzed by  $^1\text{H}$  NMR spectrometer recorded on a Lambda JEOL 400 MHz FT-NMR system with 16 scans.

### 3.3.3 Fourier Transform Infrared (FTIR) spectroscopy

The types of functional group present in the alkyd were determined by performing analysis on a Perkin Elmer Spectrum 400 FT-IR/FT-NIR Spectrometer with the attenuated total reflectance (ATR) technique. The scan recorded from 4000-450  $\text{cm}^{-1}$ .

## 3.4 Microencapsulation of pentaerythritol tetrakis, PETMP and EPON828

Dual microcapsule healing system was achieved by separately microencapsulating EPON 828 and its hardener, PETMP. Both healing agents, PETMP and EPON828 were microencapsulated by in situ polymerization. PETMP was encapsulated in Poly(melamine-formaldehyde), PMF employed from the method adopted from Yuan *et al* while microencapsulation of EPON828 in poly(urea-formaldehyde), PUF adopted from Blaiszik *et al*.

In situ polymerization techniques have been utilized for this microencapsulation. In situ polymerization or in the polymerization mixture is one of chemical microencapsulation techniques in which the polymerization of the monomer (shell forming materials) that is initially soluble occurs in the continuous phase which later deposit on the surface of the dispersed core. The core content (active healing agent) is dispersing in continuous phase forming emulsion (Ghosh, 2006; Duan, 2016).

In microencapsulation of PETMP, prepolymer of shell material was prepared by mixing 7.7 g of melamine and 14.7 g of formaldehyde in a beaker, heated at 70  $^{\circ}\text{C}$ .

The mixture was stirred continuously for 30 minutes at constant temperature. The pH of the mixture was maintained at 9 - 10 by adding triethanolamine. At the same time 50 g of PETMP was added to 2 wt% of 150 mL aqueous solution of sodium styrene maleate copolymer in a separate beaker. The reaction mixture was stirred at 600 rpm until homogeneous using a digital mixer with four-bladed, mixing propeller (MAXIMA digital, Fischer Scientific) for 30 minutes. Two drops of 1-octanol was added to the core mixture to remove bubbles. The prepolymer solution of melamine / formaldehyde was then added to the emulsion and the reaction flask was suspended in water bath. The temperature of water bath was elevated to 50 °C and stirred continuously for 3 hours. The pH of the emulsion was maintained at 3 by adding citric acid. As the reaction completed after 3 hours, the white slurry formed. The slurry formed was then cooled to room temperature followed by washing with distilled water and filtered. Dried microcapsule obtained was uniformly dispersed into N,N-dimethylbenzylamine solution at 40 °C for 24 hours. Subsequently, the microcapsule was filtered and rinsed with diethyl ether and dried at room temperature. This method was employed and modified from Yuan *et al* (Yuan *et al.*, 2008). Figure 3.2 shows the summary of microencapsulation of PETMP and the structure of PETMP was shown in Figure 3.3.



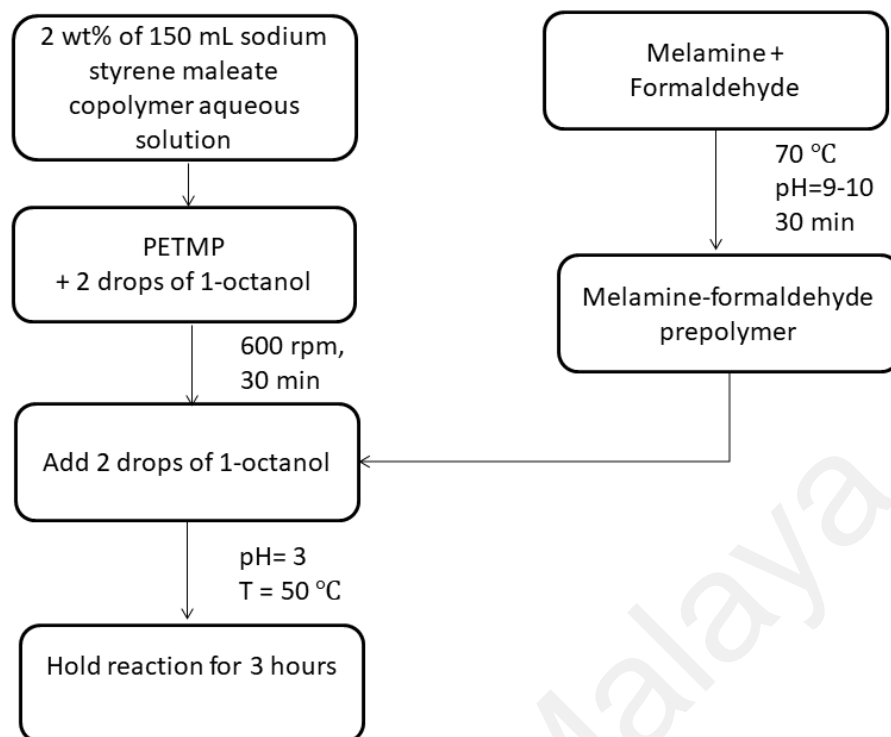


**Figure 3.2:** Summary of microencapsulation of PETMP

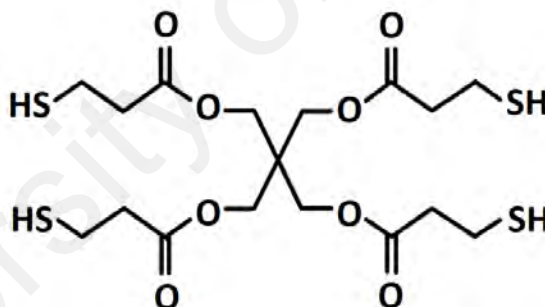


**Figure 3.3:** Structure of PETMP

Encapsulation of EPON828 proceed with method that almost similar with above procedure. Nevertheless, instead of preparing the prepolymer, the solid-wall forming materials were mixed in the reaction mixture. 2.5 g urea, 0.25 g ammonium chloride and 0.25 g resorcinol were added into 100 mL of distilled water and 25 mL of 2.5 wt% aqueous solution of EMA copolymer in a 500 mL beaker. The pH of this emulsion was adjusted to 2.7 to 3.5 by dropwise addition of 3M NaOH and 12M HCl using pH paper. The mixture was agitated driving at 450 rpm. Two drops of 1-octanol were

added to the mixture to remove bubbles. 60 mL core mixture which consists of 40 mL EPON828 in 20 mL chlorobenzene was added slowly, agitated for 10 minutes to stabilize. Polycondensation was started by adding 6.33 g formalin to the mixture, and covered with aluminium foil. The temperature of the mixture was then increased to 55 °C. The reaction was allowed to continue for 4 hours at 55°C until white slurry formed. The slurry was cooled down and washed with distilled water before filtered under suction. The free-flowing microcapsules were further dried under fan for 1 h. This method applied was modified from Blaiszik *et al* (Blaiszik *et al.*, 2009). Microencapsulation of EPON828 in chlorobenzene was summarized in Figure 3.4 while the structure of EPON828 was shown in Figure 3.5.

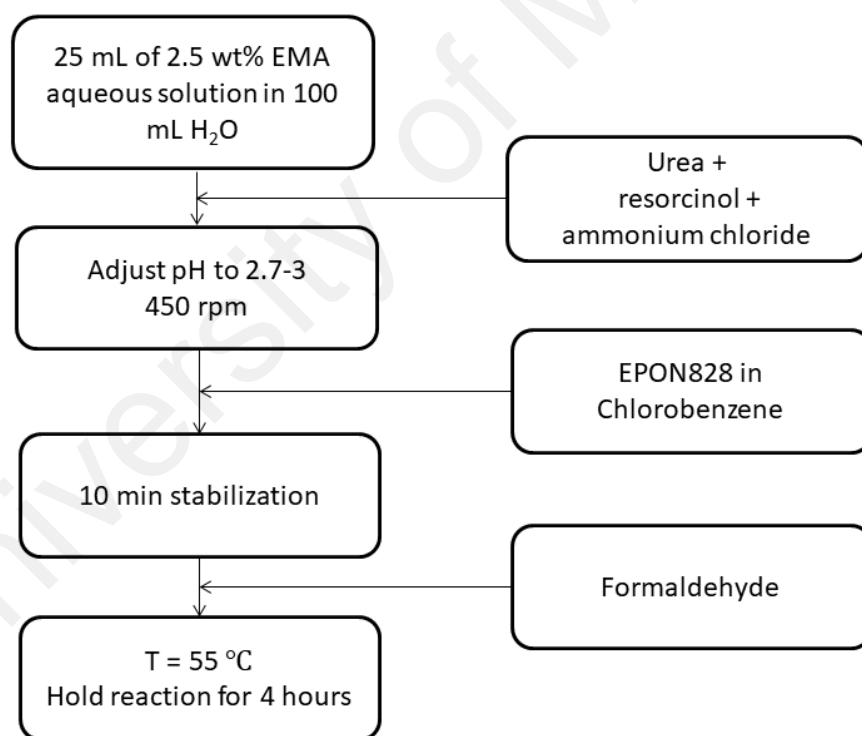


**Figure 3.4:** Summary of microencapsulation of EPON828 in chlorobenzene

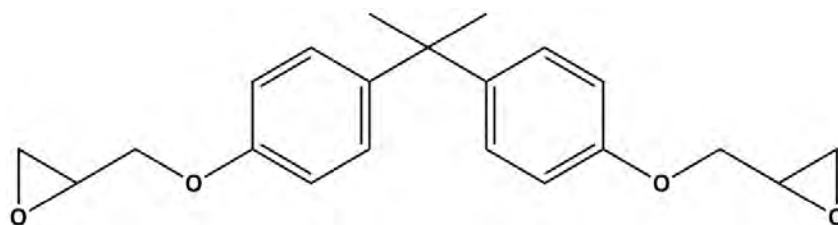


**Figure 3.5:** Structure of EPON828

### 3.4.1 Analysis of microcapsule size and surface morphology

Morphology and dimension of microcapsule was examined using Field Emission Scanning Electron Microscope (FESEM) by HITACHI UHR FESEM (SU8820 Series). Dried microcapsule was placed on a conductive carbon tape attached to a mounting piece for imaging. Microcapsule was then observed by FESEM at electron acceleration voltage of 1kV and 2kV with magnification range 150xs and 400xs.

The average diameter of dried microcapsules was determined statistically by using Image J software. The data sets of 150 individual microcapsules were obtained from the images observed under calibrated Dino-Lite digital USB microscope (AnMo Electronics) with magnification 200xs, equipped with measuring software. The area of microcapsules obtained was then calculated as follow to acquire the diameter size distribution of the microcapsules.

$$A = \frac{1}{4} \pi d^2 \quad \text{Equation 3.2}$$

Where,

A = surface area of capsule,  $\mu\text{m}^2$

d = diameter of microcapsule,  $\mu\text{m}$

### 3.4.2 Core content characterization

Core content of EPON 828 and PETMP microcapsules were analyzed to verify the success of the microencapsulation. The core content was extracted by solvent

extraction method and gravimetric analysis. Known weight of dried microcapsule ( $W_c$ ) was crushed using mortar and pestle. The core content was extracted out from shell material with acetone by filtered. The extracted core content was then left at room temperature for at least 24 hours. The residue of shell material was stirred with acetone overnight and filtered again. Filtered shell was then dried in vacuum oven at 70°C for 24 hours. The weight of final dried shell was then recorded as  $W_s$ . The extracted core content was then calculated using Equation 3.3

$$\text{Core content} = (W_c - W_s) / W_c \times 100\% \quad \text{Equation 3.3}$$

The extracted core content was analyzed using FTIR (Perkin Elmer spectrometer) and  $^1\text{H}$ - NMR (ECX400MZ-JEOL) 400 MHz spectrometer to determine the chemical structure of core monomer.

(a) ***Proton nuclear magnetic resonance ( $^1\text{H}$ -NMR) spectroscopy***

The extracted core of EPON 828 and PETMP were dissolved in deuterated chloroform ( $\text{CDCl}_3$ ) containing 99.8%  $\text{CDCl}_3$  and 0.03% tetramethylsilane (TMS) before analyzed with  $^1\text{H}$ -NMR (ECX400MZ-JEOL) 400 MHz spectrometer. The characteristic signals were processed by JEOL Resonance software and the spectra obtained were compared with spectra of pure EPON828 and PETMP for verification.

(b) ***Fourier Transform Infrared (FTIR) spectroscopy***

The extracted core of EPON828 and PETMP microcapsules were analysed on a Perkin Elmer Spectrum 400 FT-IR/FT-NIR Spectrometer with the attenuated total reflectance (ATR) technique. The spectra were recorded in the range of 4000 – 450  $\text{cm}^{-1}$  with eight scans of 4  $\text{cm}^{-1}$ . As comparison, pure EPON828 and PETMP were also analyzed to verify that EPON828 and PETMP was successfully encapsulated into poly(urea-formaldehyde) and poly(melamine-formaldehyde).

### **3.4.3 Thermal analysis of microcapsule**

Thermal analyses of microcapsules were analyzed via differential scanning calorimetry (DSC) and thermogravimetric analysis (TGA). DSC analysis was conducted using DSC TA Instrument (Model: Q20). Both EPON828 and PETMP microcapsules, their extracted core and shell materials were measured at heating rate 10°C/min from 25°C to 400°C. For thermogravimetric measurement, the samples were then measured using TGA 6, Perkin Elmer in nitrogen atmosphere with heating rate maintained at 10 °C/min from 25°C to 900°C.

### **3.5 Preparation of coating mixture**

UV-curable self-healing coating was prepared by synthesizing palm oil-based alkyd which serves as coating binder, microencapsulation of healing agents, and preparation of coating mixture and rendered under UV radiation. Apart from alkyd, the coating mixture includes microcapsules that contain healing agents, methyl methacrylate as reactive diluents and benzophenone as UV photoinitiator.

Self-healing coating was prepared at ambient temperature by dissolving 3 parts of alkyd to 2 parts of MMA by mass. MMA was used in this coating mixture as reactive diluents. 6 parts per hundred parts (pphr) of benzophenone was added as photoinitiator. The mixture was stirred until homogeneous before the microcapsule was added. The mixture was then swirled slowly to let the microcapsule dispersed uniformly in the coating mixture.

#### **3.5.1 Treatment of mild steel plate**

Iron panels that were used as a substrate for coating were cleaned initially before being applied by coating mixture. The plates were degreased with toluene to remove any stains and impurities followed by acetone. It was then abraded using abrasive

paper with grain size P600 to P1600. The acetone was used once again to remove dust and the mild steel was kept in drying cabinet.

### **3.5.2 Coatings application and curing**

The coating mixtures were applied onto the mild steel by using bar coater and irradiated with UV light (Electro-Lite Corporation (Electro-Cure 4001) immediately to cure. The UV light radiated at  $\lambda=365$  nm with intensity of  $125 \text{ Mw/cm}^2$ . The coated mild steel was then inspected physically to determine their dry-hard and tack-free state. Based on ASTM D1650-91, the condition of the coating film is considered as dry-hard when there is no marking or the marking on the film disappear by light polishing as pressure was applied by using thumb. The coating is considered as tack free as the film is no longer tacky when touches. The dried thickness of coatings was measured using Mitutoyo Digital Micrometer Gauge for four times. The average thickness of the coating was calculated and recorded as  $132.4 \pm 12.1 \text{ }\mu\text{m}$ .

### **3.5.3 Evaluation of amount of microcapsules loading on self-healing ability**

Self-healing coating with different amounts of microcapsule was prepared to evaluate the sufficient amount of microcapsules needed for the coating to be able to self-heal. In general, higher amount of microcapsules in the coating will increase the efficiency of self-healing owing to higher amount of microcapsule present at damage site. Hence, this evaluation was conducted to determine the minimum amount of microcapsules needed for the coating to be able to self-heals. Self-healing coatings were prepared with different amounts of microcapsules ranging from 3.0, 5.0 and 7.0 wt% (with 1:1 ratio of microcapsules of PETMP to EPON828). The microcapsules were then added into the coating mixture and stirred uniformly. The coating mixture was then applied onto the mild steel and irradiated with UV light to cure. The coated mild steel was purposely scribe and observed under calibrated digital microscope.

#### **3.5.4 Evaluation of amount of microcapsule on adhesion properties of film on the substrate**

In relation with the Section 3.5.3, the adhesion property of film of the coating is inversely proportional to the amount of loading of microcapsule in the coating. The higher the amount of microcapsule reduces the adhesion strength of film onto the substrate due to the presence of larger amount microcapsule. Hence, the adhesion test was carried out to determine the limit of the microcapsule's loading. In this examination, coating with higher loading of microcapsule was prepared ranging from 7.0, 9.0, 11.0, 13.0 and 15.0 wt%. The coating was scribe in accordance to ASTM D3359-02 and the detail of the test was described in Section 3.7.1. Note that the test was carried out immediately after scribe. The coating with excellence adhesion strength and able to self-heal was chosen for the next evaluation of self-healing coating.

#### **3.6 Analysis of crosslink reaction between EPON828 and PETMP**

The time needed for the healing reaction (reaction between EPON828 and PETMP in the presence of catalyst) to solidify upon crosslinked was investigated by physical evaluation and FTIR analysis. Both evaluations were conducted at the same time. EPON828 and PETMP were mixed with ratio 1:1 in the presence of N,N-dimethylbenzene as catalyst. Upon mixing, the small amount of reaction mixture was taken out and analysed by FTIR spectroscopy repeatedly and at the same time, the reaction mixture left was inspected physically. The analyses and inspection were continued until the reaction mixture was hardened. The time of every FTIR analyses and time needed for the reaction mixture to solidify were recorded. This evaluation was conducted to predict the reaction time of healing agents when introduced into the coating matrix.

### **3.7 Coating film properties**







The physical and chemical properties of the coating was investigated by conducting the following tests. Every tests was performed on a dried test specimens that involves two types of coating which is self healing coating and alkyd coating without loaded microcapsule as a control. The purpose of the control is to determine if any depreciation in the film properties arise when microcapsules were loaded into the coating.

#### **3.7.1 Film adhesion tape test**

Film adhesion test was conducted following ASTM D3359-02. Dry thickness of the coated film was measured using Mitutoyo Digital Micrometer Gauge at four separate points and the average thickness of the coating was recorded. The thickness of the coating was needed to determine the film adhesion test method. The procedure of the test proceeds according to ASTM D3359-02 Method A. An X- cut consisting of 40 mm intersecting in their middle was carved on the coating using a blade. A 75 mm long self-adhesive tape was placed on the intersection of the cut. The area of the incision was gently rubbed using an eraser to ensure good contact between the tape and the film. The tape was then removed rapidly at an angle close to 180° with single stroke and the X-cut area was inspected for any removal of the coating. The result of film adhesion tape test were classified as shown in Table 3.1.



**Table 3.1:** Classification of coating area removal

Classification	Coating removed	Surface of X-cut area
5A	None	
4A	Trace along incision	
3A	<1.6 mm along incision	
2A	1.6 mm – 3.2 mm along incision	
1A	Most of the area of X	
0A	Beyond the area of X	

### **3.7.2 Water and alkali resistance test**

Water and alkali resistance tests were conducted on coated glass panels using methods adopted from ASTM D1647-89. In water resistance test, the coated glass panels were immersed in distilled water at ambient temperature after cured with UV light. The glass panel was removed after 24 hours and inspected visually for any film defect. If whitening formed upon removing the glass panels, the coating was dried at room temperature and the time needed for the whitening to disappear during the drying time was recorded.

Alkali resistance test was conducted by soaking the coated glass panel in NaOH aqueous solution (30 g/L). Film condition of the coatings was checked after every 5 minutes of immersion. The alkali resistance was determined by the time of the immersion needed for the film defect to be visible. The coating is considered to have high resistance of alkali if longer time is needed for the film defect to appear during the immersion. The tests were also conducted on glass panel with alkyd coating which serve as control sample.

### **3.7.3 Acid resistance test**

Acid resistance test was performed by immersing the coated glass panels in 0.1M HCl solution. The solution was preheated at 80°C and the temperature was maintained throughout the immersion for 1 hour by using water bath. The coated glass panels were then removed and rinsed with distilled water. Any films defect was observed after dried for 24 hours at room temperature (Ang, 2012).

### **3.7.4 Salt water resistance test**

Salt water resistance test was conducted as similar as procedure in Section 3.7.3. Coated glass panels were immersed in 5 wt% aqueous NaCl solution in which this solution was preheated at 80 °C. The temperature was maintained at 80 °C throughout

the test for 1 hour in water bath. The glass panels were then removed and dried for 24 hours at room temperature. Any blemish on the film of the glass panels was visually inspected.

### **3.8 Corrosion study**

#### **3.8.1 Basic corrosion test**

The self-healing efficacy of the coating was evaluated by performing basic corrosion test on the coating applied on mild steel plate. After irradiated under UV-light, the dried self-healing coating was hand-scratched by using a razor blade. The coating was then left at room temperature for 24 hours to self-heal. The coated steels were then immersed in 3.5 wt% NaCl solution for 24 hours and subsequently inspected visually and observed under calibrated digital microscope (AnMo Electronics, Taipei, Taiwan). Alkyd coating without microcapsules was used as control.

#### **3.8.2 Potentiodynamic polarization test**

Anti-corrosion property of self-healed alkyd coating was also investigated quantitatively by electrochemical test performed using AUTOLAB Potentiostat/Galvanostat PGSTAT302N (Ecochemie, Netherlands). Coated specimen was scribed and allowed to self-heal for 24 hours. The coated specimen was then attached to the electrochemical cell which consist of 2 cm X 7 cm (diameter x length) glass tube shown in Figure 3.6 using Araldite High Performance Epoxy Adhesive. The glass tube was filled with 3.5 wt% NaCl solution and left for 1 hour to equilibrium followed by potentiodynamic polarization test with three-electrode setup (Figure 3.7). The mild steel served as working electrode while platinum wire as counter electrode and Ag/AgCl (saturated KCl) used as reference electrode. This experiment was measured between -1 to +1 V with 1 mV/s scan rate. The Faraday's Law was applied

in the analysis and the corrosion rate was calculated using Equation 3.4 (Stansbury & Buchanan, 2000):

$$\text{CPR} = \frac{3.27 i_{corr} (EW / \rho)}{3.4} \quad \text{Equation 3.4}$$

Where,

CPR = corrosion penetration rate (mm/y)

$i_{corr}$  = corrosion current density (mA/cm<sup>2</sup>)

EW = equivalent weight of metal (g)

$\rho$  = density of metal (g/cm<sup>3</sup>)



**Figure 3.6:** Coated mild steel attached with electrochemical cell

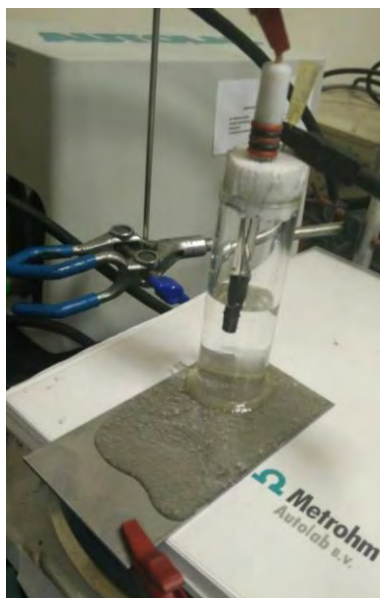


**Figure 3.7:** Set of electrochemical test with three-electrode setup

## CHAPTER 4: RESULTS AND DISCUSSION

### 4.1 Synthesis of alkyd

Alkyd synthesis involves alcoholysis of oil and polyesterification process between monoglycerides with diacids. The alkyd produced was dark brown in colour and very viscous.

### 4.2 Characterization of alkyd

#### 4.2.1 Acid number

The initial acid number of alkyd was 213 mgKOH/g alkyd when calculated theoretically. The acid number was measured after every one hour interval. As the reaction continued, the acid number decreased owing to the conversion of  $\text{-COOH}$  into ester linkages. The acid number decline rapidly at the initial phase of reaction since the reaction mixture has more of  $\text{-COOH}$  and  $\text{-OH}$  present, which then reduced slowly as the concentration of functional groups decreased (Ang, 2012). The reaction was carried on until the acid number dropped to below 10% from initial, which is the final acid number is 16.4 mgKOH/g. A notable increase in viscosity of the alkyd is observed when the acid number is sufficiently low. This is due to increasing amount of free fatty acid crosslinked. Higher viscosity of alkyd is needed in this work as it will provide a coating matrix with well dispersed of microcapsule. The incorporation of maleic acid in the alkyd synthesis increase the unsaturation of fatty acid in the presence of  $\text{-CH=CH-}$ , which is crucial for rapid curing and improved physicochemical properties (Ang & Gan, 2012a).

#### 4.2.2 $^1\text{H-NMR}$ spectroscopy

Figure 4.1 shows the  $^1\text{H-NMR}$  spectra of alkyd and palm olein. The peaks assignment is given in detail and shown in Table 4.1. In Figure 4.1 (b), the resonance peaks of allylic and vinylic protons of oleic and linoleic acid for palm olein oil

observed at peaks 2.00 and 5.34 ppm. The peaks at 0.88 and 1.26 ppm attributed to methyl and methylene protons from the hydrocarbon chain of fatty acid. The methylene proton of ester chain was observed at peaks 1.6 and 4.10-4.30 ppm.

On the other hand, peaks at downfield region with chemical shift of  $\delta = 7.50$  and 7.70 ppm only appear at  $^1\text{H}$ -NMR spectrum of alkyd in Figure 4.1 (a) indicate the aromatic protons that presence from the phthalic anhydride. Meanwhile, peak at  $\delta = 6.85$  ppm attributed to the  $\text{OOC}-\text{CH}=\text{CH}-\text{COO}$  from the maleic acid moiety of the alkyd.

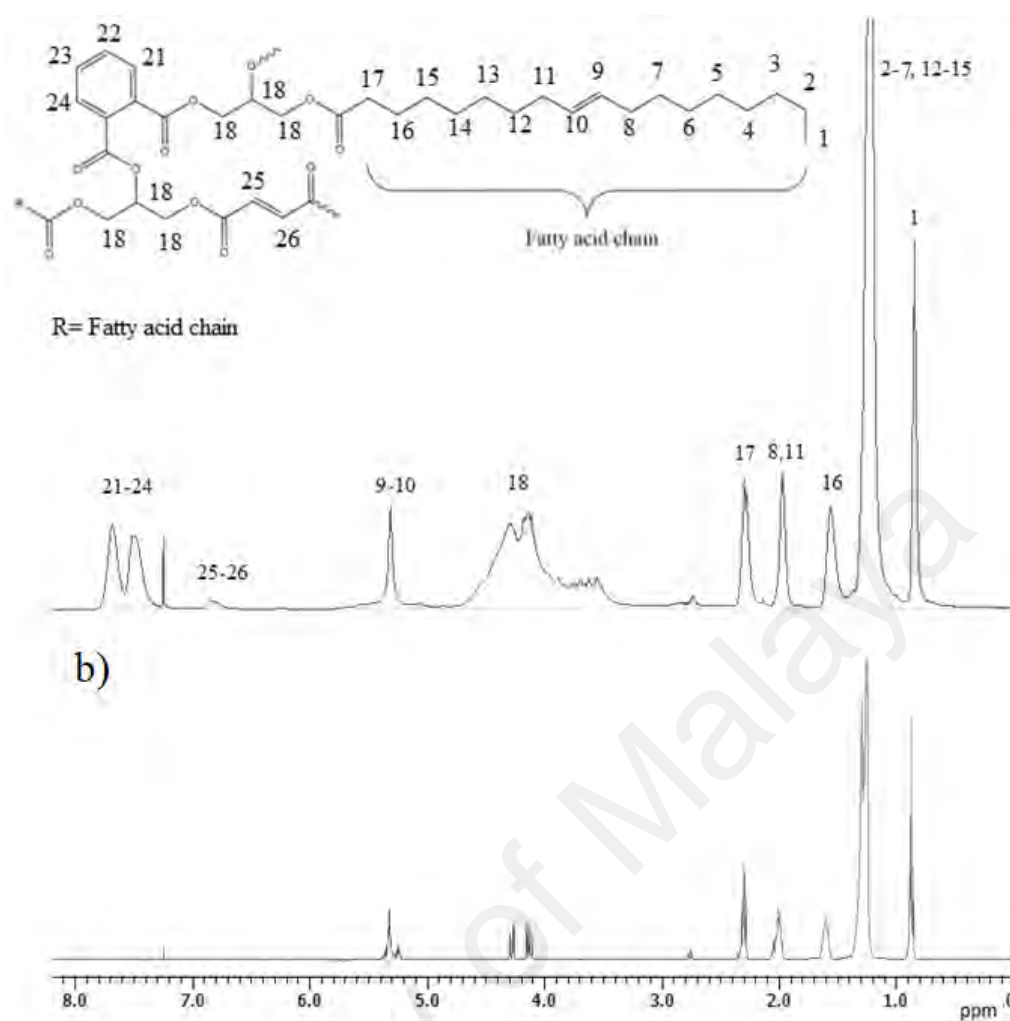


**Figure 4.1:**  $^1\text{H}$ -NMR spectra of (a) alkyd, (b) palm olein [Inset shows the structure of alkyd]



**Table 4.1:** Peak assignments for  $^1\text{H}$ -NMR spectra of alkyd and palm olein.

Alkyd		Palm olein	
Chemical shifts ( $\delta$ ) / ppm	Proton assignment	Chemical shifts ( $\delta$ ) / ppm	Proton assignment
0.88	$\text{CH}_3$	0.88	$\text{CH}_3$
1.26	$-\text{R}-\text{CH}_2-\text{R}$	1.26	$-\text{R}-\text{CH}_2-\text{R}$
1.60	$-\text{OOC}-\text{CH}_2-\text{CH}_2-$	1.60	$-\text{OOC}-\text{CH}_2-\text{CH}_2-$
2.00	$-\text{R}-\text{CH}_2-\text{CH}=\text{CH}-$	2.00	$-\text{R}-\text{CH}_2-\text{CH}=\text{CH}-$
2.30	$-\text{OOC}-\text{CH}_2-$	2.30	$-\text{OOC}-\text{CH}_2-$
4.10-4.30	$-\text{COO}-\text{CH}_2-$	4.10-4.30	$-\text{COO}-\text{CH}_2-$
5.34	$-\text{HC}=\text{CH}-$	5.34	$-\text{HC}=\text{CH}-$
6.85	$-\text{OOC}-\text{CH}=\text{CH}-\text{COO}-$	-	-
7.50, 7.70	Aromatic $-\text{CH}=\text{CH}$	-	-

#### 4.2.3 FTIR spectroscopy

The FTIR spectra of alkyd and palm olein are shown in Figure 4.2 and peaks assignment are summarised in Table 4.2. New broad band of peaks in alkyd spectrum was observed at  $3458\text{ cm}^{-1}$  and  $1600\text{ cm}^{-1}$  due to O-H stretching formed and aromatic  $-\text{CH}=\text{CH}$  from the phthalic acid, respectively. Sharp peaks at  $2923$  and  $2854\text{ cm}^{-1}$  correspond to C-H stretching, and a strong peak at  $1772\text{ cm}^{-1}$  represents C=O carbonyl groups. An aromatic ring was observed at peak  $1600\text{ cm}^{-1}$ , and C-H and C-R bending modes at peak  $1454$  and  $1373\text{ cm}^{-1}$ , respectively. Peaks for C-O groups were observed at  $1070$ ,  $1120$  and  $1260\text{ cm}^{-1}$ . Peak at  $742\text{ cm}^{-1}$  was attributed to aromatic  $=\text{C}-\text{H}$  bending.

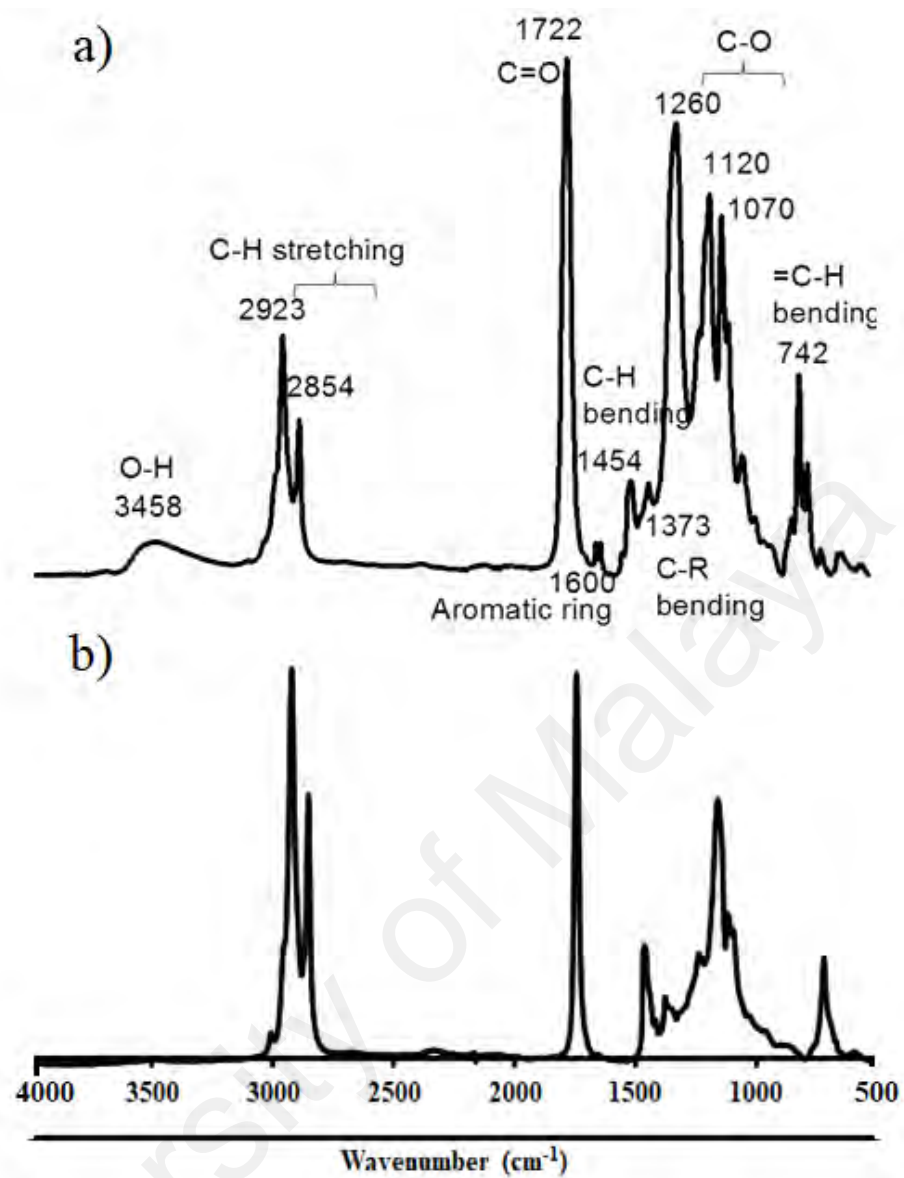


**Figure 4.2:** FTIR spectra of (a) alkyd, (b) palm olein [Inset shows the structure of alkyd]

**Table 4.2:** FTIR assignment peaks for alkyd and palm olein oil.

Alkyd		Palm olein	
Wavenumber / (cm <sup>-1</sup> )	Functional group	Wavenumber / (cm <sup>-1</sup> )	Functional group
3458	O-H stretching	-	-
2923, 2854	C-H stretching	2923, 2853	C-H stretching
1772	C=O carbonyl groups	1744	C=O carbonyl groups
1600	Aromatic ring	-	-
1454	C-H bending	1466	C-H bending
1373	C-R bending	1379	C-R bending
1260, 1120, & 1070	C-O groups of ester	1160, 1118	C-O stretching
742	Aromatic =C-H bending	722	-CH <sub>2</sub> rocking

### 4.3 Synthesis of microcapsules

The microcapsules produced were free-flowing and spherical in shape. In microencapsulation of PETMP, PMF was used as shell material due to its inertness towards mercaptan. Mercaptan is highly reactive due to the high activity of hydrosulfide group (Yuan *et al.*, 2008). Since PMF wall has high chemical and mechanical stability, thus PMF is suitable to encapsulate PETMP. The reaction takes places in two stages which involved preparation of melamine-formaldehyde prepolymer and polycondensation. Melamine-formaldehyde prepolymer was prepared in basic condition by nucleophilic addition at 70 °C. Different ratio of formaldehyde-to-melamine produced different types of initial products ranging from mono- to

hexamethylolmelamines (Zhang & Rong, 2011). In this case, hexamethylolmelamines was produced from the ratio of formaldehyde-to-melamine of 9. This is due to high stability of hexamethylolmelamine and its further condensation produced high molecular weight and superior strength of MF resin (Palanikkumaran *et al.*, 2009). The prepolymer was then preceded with polycondensation stage which occurs simultaneously with in situ polymerization reaction. In contrast with nucleophilic addition, polycondensation reaction was prepared in acidic condition at 50 °C. During polycondensation reaction, ether bridges between the reaction of two methylol groups, and methylene bridges between methylol and amino groups were formed. At the same time, the prepolymer and melamine-formaldehyde monomer reacted together forming low molecular weight oligomers during in situ polymerization since they possess surface activity like surfactant. The hydrophilic and hydrophobic interaction of tenside molecules concentrated the oligomers, thus enhanced the wall formation (Dietrich *et al.*, 1990). Figure 4.3 shows the reaction scheme of melamine-formaldehyde resin formation adopted from the work of Yuan et al.

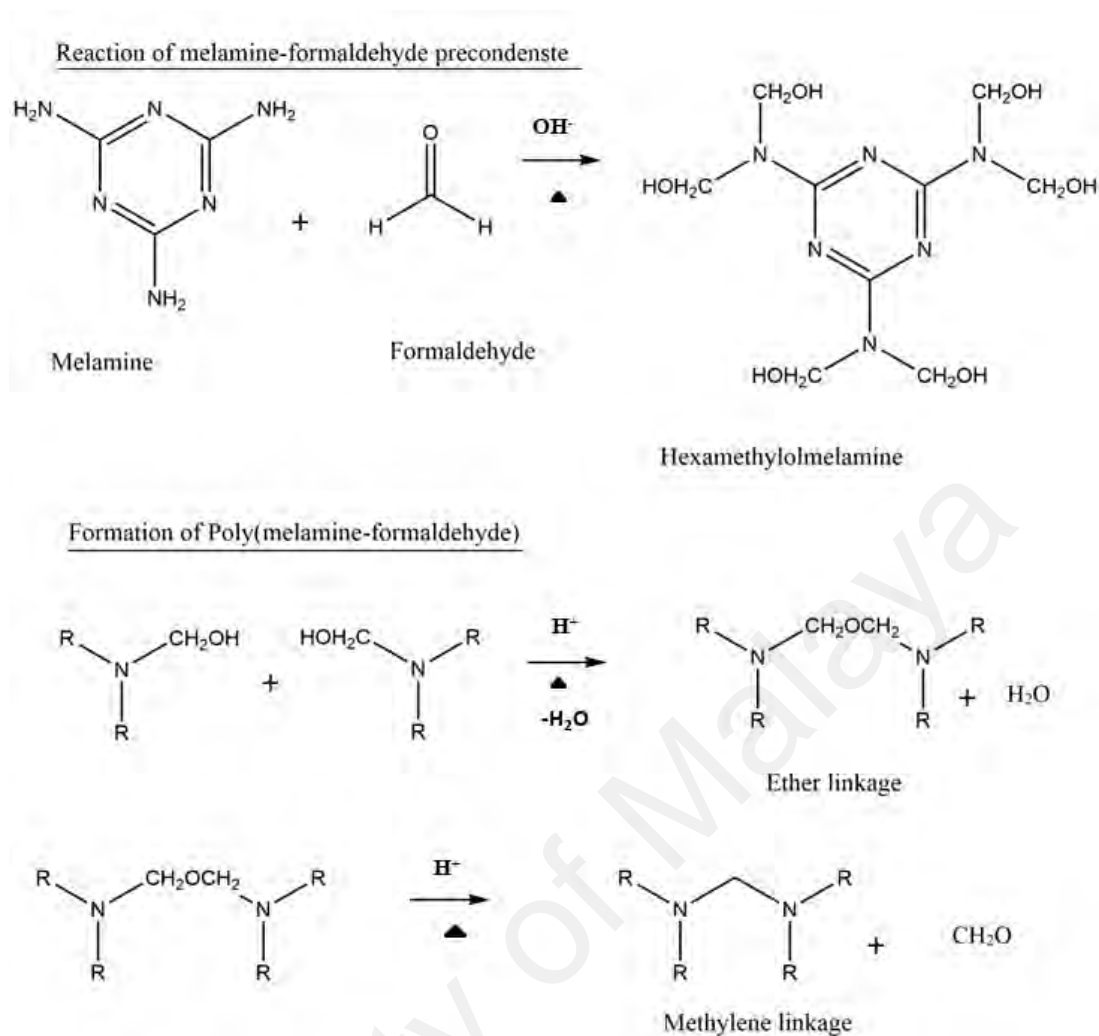


**Figure 4.3:** Reaction scheme of melamine-formaldehyde

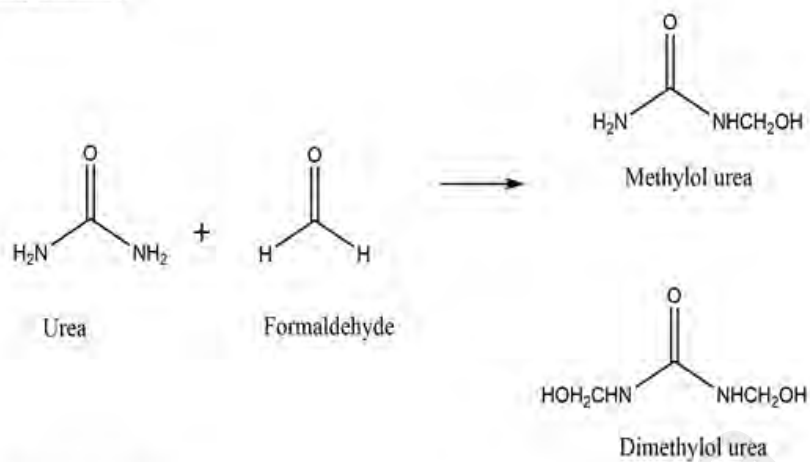
Microencapsulation of EPON 828 in poly(urea-formaldehyde) was done by in situ polymerisation. The emulsion takes place when EPON 828 was dispersed in water that contains surfactant and physical stirring of the emulsion forms droplet of EPON828. Reaction between urea and formaldehyde forms methylol urea. Similar to microencapsulation of PETMP, polycondensation of urea and formaldehyde takes place in acidic condition at 55 °C. As the solution become acidic, the methylol urea becomes more hydrophobic. This is due to the formation of methylene bridge and ether linkage from the reaction between methylol urea and amino groups. At the phase boundary, the oligomers become more concentrated and forming primary wall on the oil droplet. This phenomenon owing to the interactions occurs between hydrophilic

and hydrophobic. The primary wall formed undergoes further crosslinking via polycondensation and this helps to build up the thickness of the wall (Duan, 2016).

Figure 4.4 shows the reaction scheme of urea-formaldehyde resin formation.

University of Malaya

### Methylation



### Polycondensation

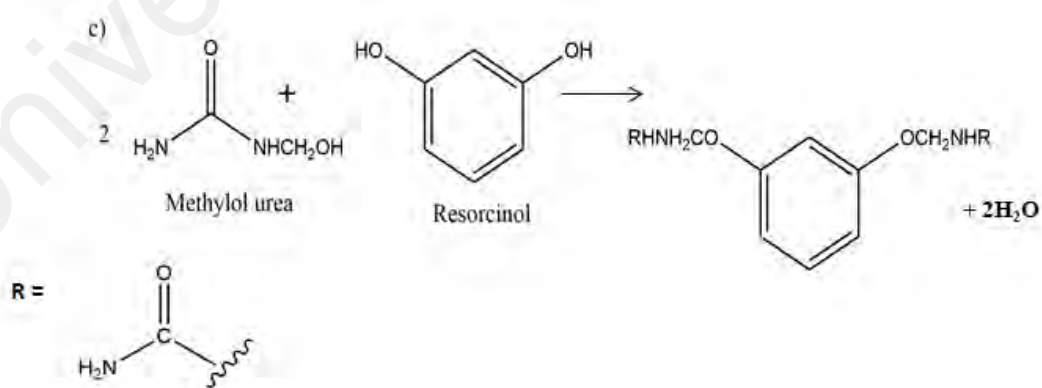
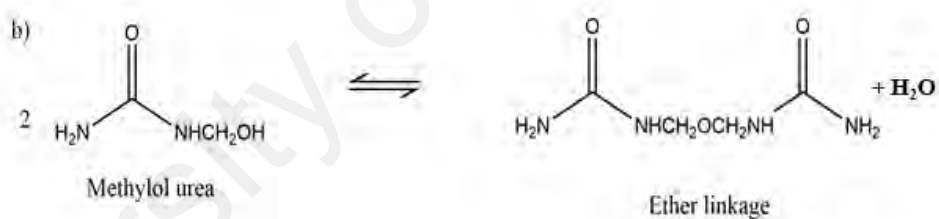
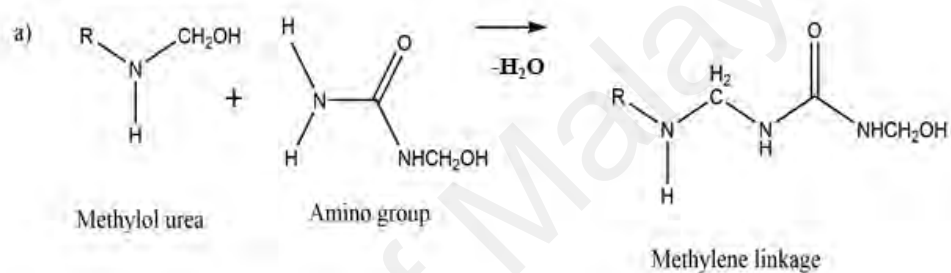


**Figure 4.4:** Reaction scheme of urea-formaldehyde

#### 4.3.1 Surface morphology and size distribution

Figure 4.5 shows the morphology of EPON 828 microcapsules while Figure 4.6 shows the morphology of PETMP microcapsules captured using FESEM and calibrated digital microscope, as well as their size distribution. The microcapsules have rough surface which is desirable as it could improve the surface interaction between microcapsule and the coating matrix. The size distribution was analysed from the digital microscope. Both microcapsules have almost same average diameter size in which the largest number of both microcapsules is in the diameter range of 111-130  $\mu\text{m}$ .

Both microcapsules are intentionally ruptured using a fine blade observed under digital microscope as shown in Figure 4.7 and Figure 4.8. Fluid exudes out from the ruptured microcapsules are presumed to be encapsulated EPON828 and PETMP, and this serves as a primitive evident that the healing agents were successfully microencapsulated. The core contents of the microcapsules were subjected to spectroscopic analysis to confirm the success of the microencapsulation.



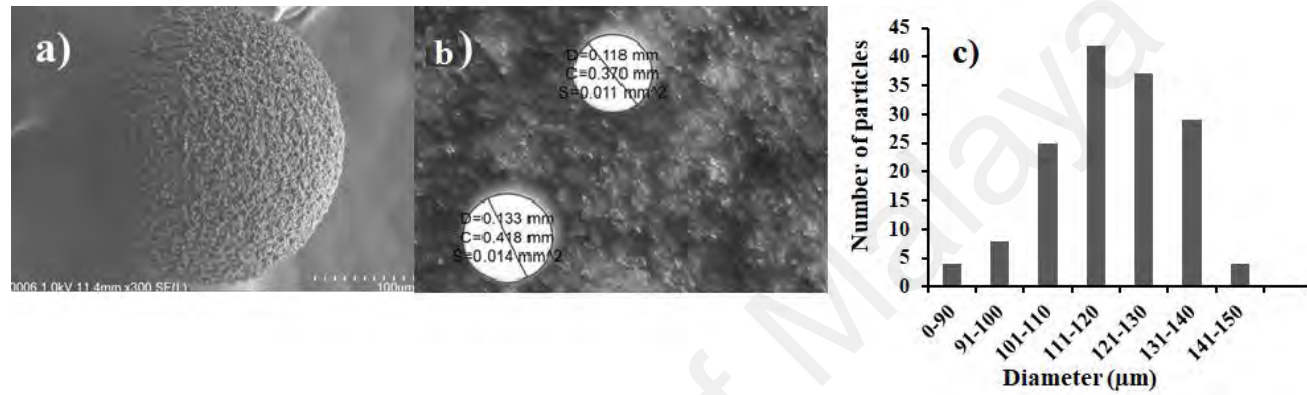


**Figure 4.5:** Image of EPON 828 microcapsule observed under a) FESEM, b) digital microscope and c) its size distribution

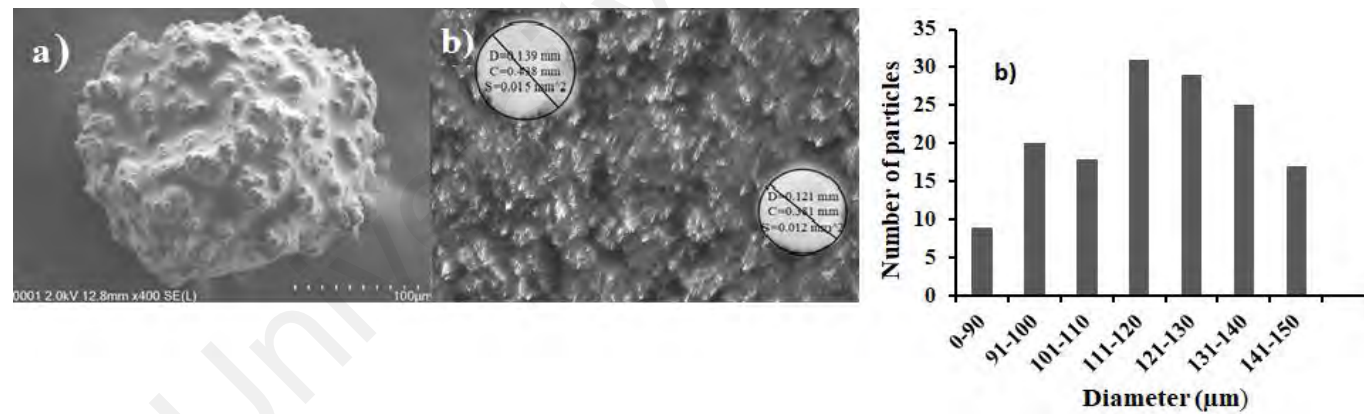


**Figure 4.6:** Image of PETMP microcapsule observed under a) FESEM, b) digital microscope and c) its size distribution

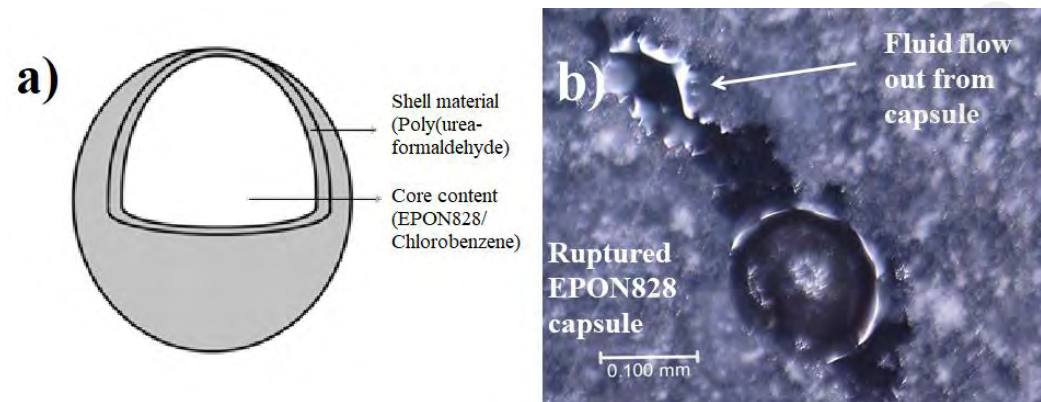


**Figure 4.7:** (a) Anatomy of EPON828 microcapsule, (b) image of ruptured EPON 828 microcapsules observed under digital microscope

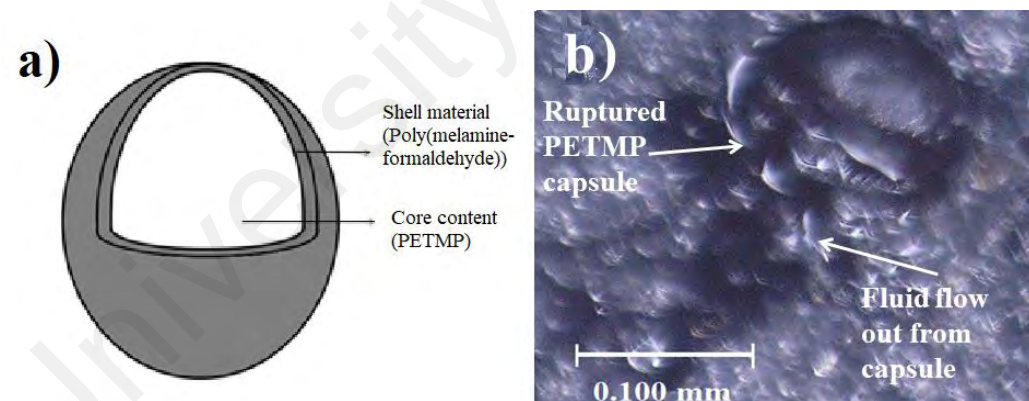


**Figure 4.8:** (a) Anatomy of PETMP microcapsule, (b) image of ruptured PETMP microcapsules observed under digital microscope

#### 4.3.2 Core content analysis

The core contents of both microcapsules were extracted by solvent extraction method. The extent of the microencapsulation calculated based on the amount of extracted core content is quite promising, with percentage of microencapsulation of EPON828 and PETMP reached as high as 89 and 87% respectively. Structural analysis was conducted by performing  $^1\text{H}$ -NMR and FTIR analyses to identify the core content extracted from both series of microcapsules. The spectra of the core content were compared to those of neat EPON828 and neat PETMP. Note that neat of EPON828 and PETMP are the pure liquid of EPON828 and PETMP without being encapsulated.

##### (a) *EPON828 microcapsule*

Figure 4.9 shows the comparison of  $^1\text{H}$ -NMR spectra between neat EPON828 and extracted core content. Both peaks in the  $^1\text{H}$ -NMR spectra of extracted core of EPON828 microcapsules and neat EPON828 resemble one another, and this indicates successful microencapsulation of EPON828. Note that peaks that correspond to chlorobenzene was not observed in the spectrum of extracted core due to the fact that solvent has evaporated off during the drying stage in the solvent extraction method. Thus, the extracted core was compared with neat EPON828 only without the presence of chlorobenzene. The summary of assignment peaks is displayed in Table 4.3.

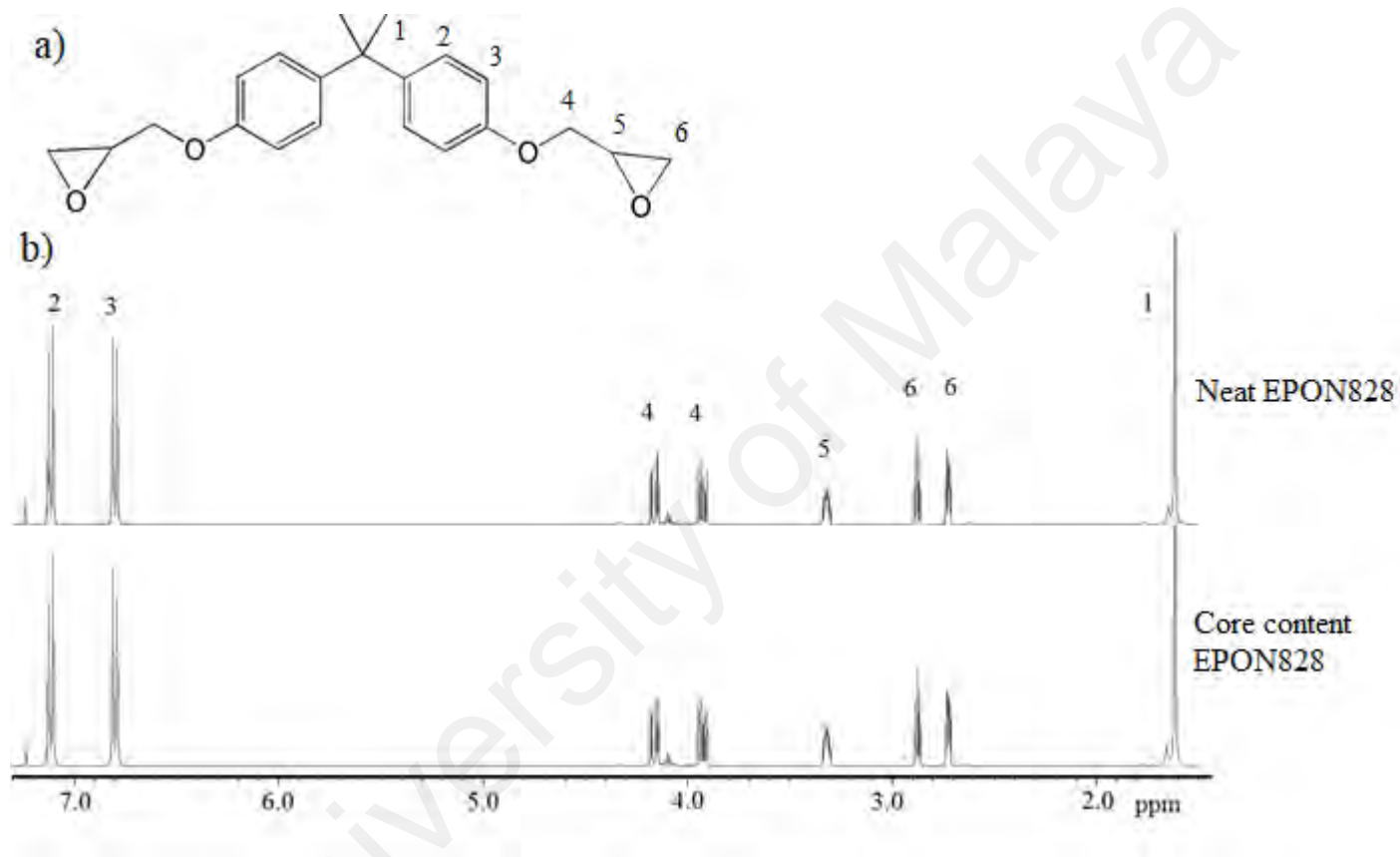


**Figure 4.9:** (a) Chemical structure of EPON828, (b)  $^1\text{H}$ -NMR spectra of neat EPON828 and extracted core of EPON828

**Table 4.3:** The chemical shift of the peaks present in  $^1\text{H}$ -NMR spectra of EPON828

Chemical shifts ( $\delta$ ) / ppm	Proton assignment
1.61	$\text{CH}_3$
6.80	Hydrogen resonance of aromatic ring
7.11	Hydrogen resonance of aromatic ring
3.91-3.95	$\text{O-CH}_2$
4.08-4.18	$\text{O-CH}_2$
2.72-2.73	$\text{CH}_2\text{-O-CH}$ , oxirane group
2.86 - 2.89	$\text{CH}_2\text{-O-CH}$ , oxirane group
3.31-3.32	$\text{CH-O-CH}_2$ , oxirane group

Similar with extracted core content of EPON828 microcapsule, the spectrum of extracted core of EPON828 capsule is identical with the spectrum of neat EPON828. The infrared spectrum of core content of EPON828 as shown in Figure 4.10. When comparing the spectra of core content of EPON828 with neat EPON828 as reference, all the characteristic peaks are present. Peak at  $3504\text{ cm}^{-1}$  indicate the presence of OH group, peak at  $862\text{ cm}^{-1}$  represent epoxy ring stretch and  $832\text{ cm}^{-1}$  represent out of plane bending of the aromatic ring.

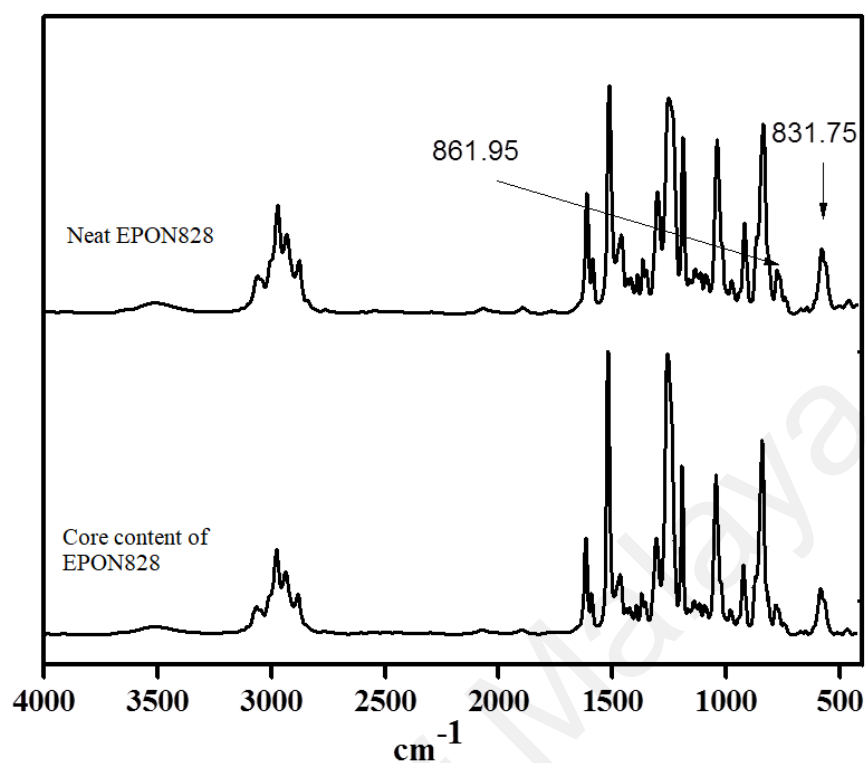


**Figure 4.10:** FTIR spectra of neat EPON828 and core content EPON828

(b) *PETMP microcapsule*

$^1\text{H}$ -NMR spectrum of extracted core content of PETMP microcapsules was compared with the spectrum of neat PETMP in Figure 4.11. The peaks that appear in both spectra of neat PETMP and core content of the PETMP microcapsule are identical. This verifies that the microencapsulation of PETMP was successful. The assignment peaks of PETMP displayed in Table 4.4.

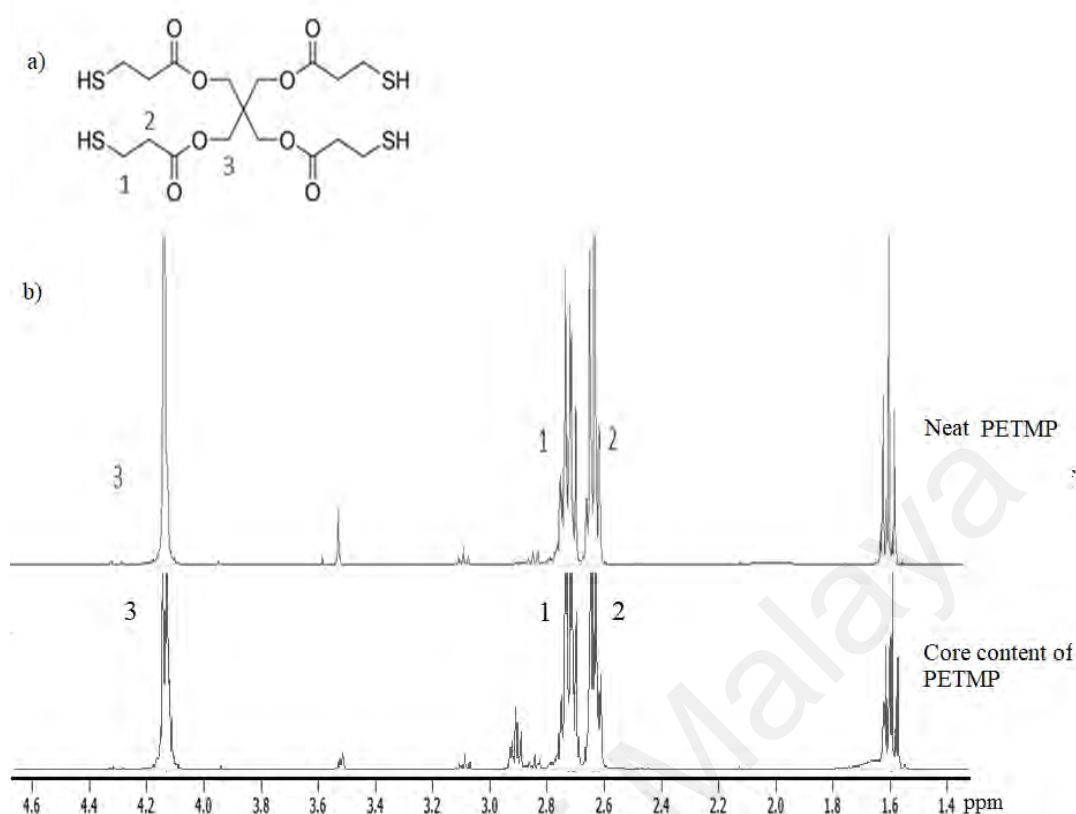


**Figure 4.11:** (a) Chemical structure of PETMP, (b)  $^1\text{H}$ -NMR spectra of neat PETMP and extracted core of PETMP

**Table 4.4:** The chemical shift of the peaks present in  $^1\text{H}$ -NMR spectra of PETMP

Chemical shifts ( $\delta$ ) / ppm	Proton assignment
2.62-2.69	$\text{CH}_2\text{-COO}$
2.71-2.78	$\text{HS-CH}_2$
4.16	$\text{-COO-CH}_2$

The FTIR spectra of the extracted core content of PETMP microcapsules, and neat PETMP reference were compared and shown in Figure 4.12. The comparison reveals that all the peaks that are present in the FTIR spectrum of the core content of the microcapsules correspond to peaks present in spectrum of neat PETMP. The result is in agreement with  $^1\text{H}$ -NMR analysis, suggesting successful microencapsulation of PETMP. Thus, it verified that PETMP was successfully encapsulated. Peak at 2571

$\text{cm}^{-1}$  shows the S-H vibration and peak at  $1731\text{ cm}^{-1}$  correspond to C=O vibration of ester group.

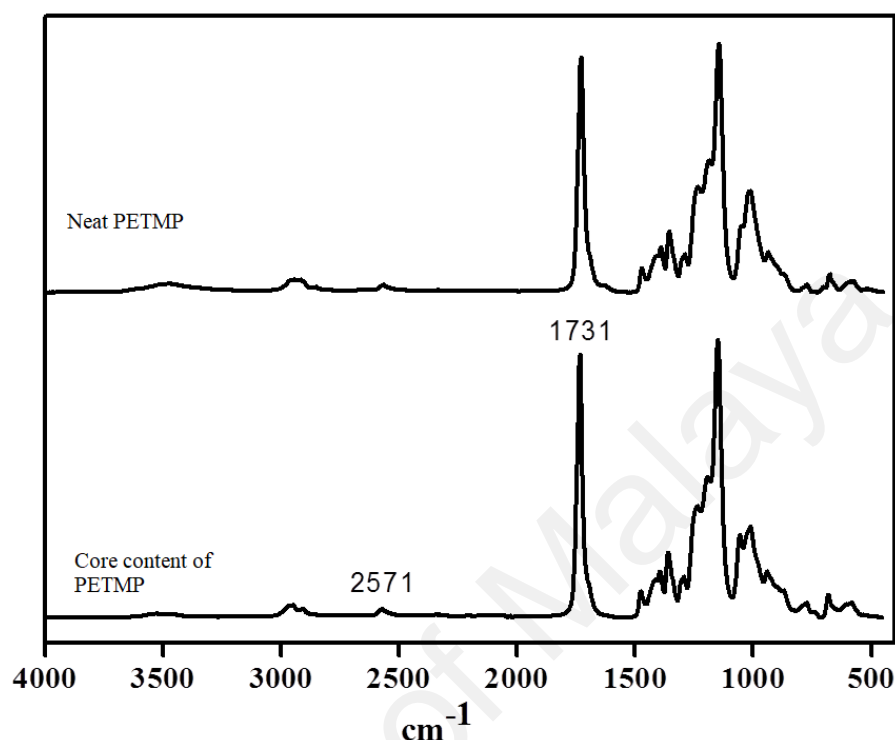


**Figure 4.12:** FTIR spectra of neat PETMP and core content of PETMP

### 4.3.3 Thermal analysis of microcapsules

#### (a) *EPON828 microcapsule*

Thermal analysis of microcapsule, extracted core and shell materials were recorded in the following figure. The thermal analysis were analysed using differential scanning calorimetry (DSC) from  $25\text{ }^{\circ}\text{C}$  to  $400\text{ }^{\circ}\text{C}$  and thermogravimetric analysis (TGA) from  $25\text{ }^{\circ}\text{C}$  to  $900\text{ }^{\circ}\text{C}$  and. From the DSC thermogram of EPON828 in Figure 4.13 (a), the glass transition temperature,  $T_g$  for shell material is recorded at  $128\text{ }^{\circ}\text{C}$  followed, by melting endotherm at  $166\text{ }^{\circ}\text{C}$ . The shell softens and releases the core content when surpass the  $T_g$  of the microcapsule. The exothermic peaks are observed at temperature exceeded  $220\text{ }^{\circ}\text{C}$  which correspond to homopolymerization of EPON828.



Thermal degradation of EPON828 microcapsule, shell and extracted core was observed in Figure 4.13 (b). At temperature near 100 °C, the shell material curve shows weight lost which attributed to the entrapped residual water and the free formaldehyde. The capsule starts to show weight loss at 238-300 °C which corresponds to the evaporation of exuded EPON828. The boiling point of EPON828 reported at 260 °C (Momentive, 2015).

University of Malaya

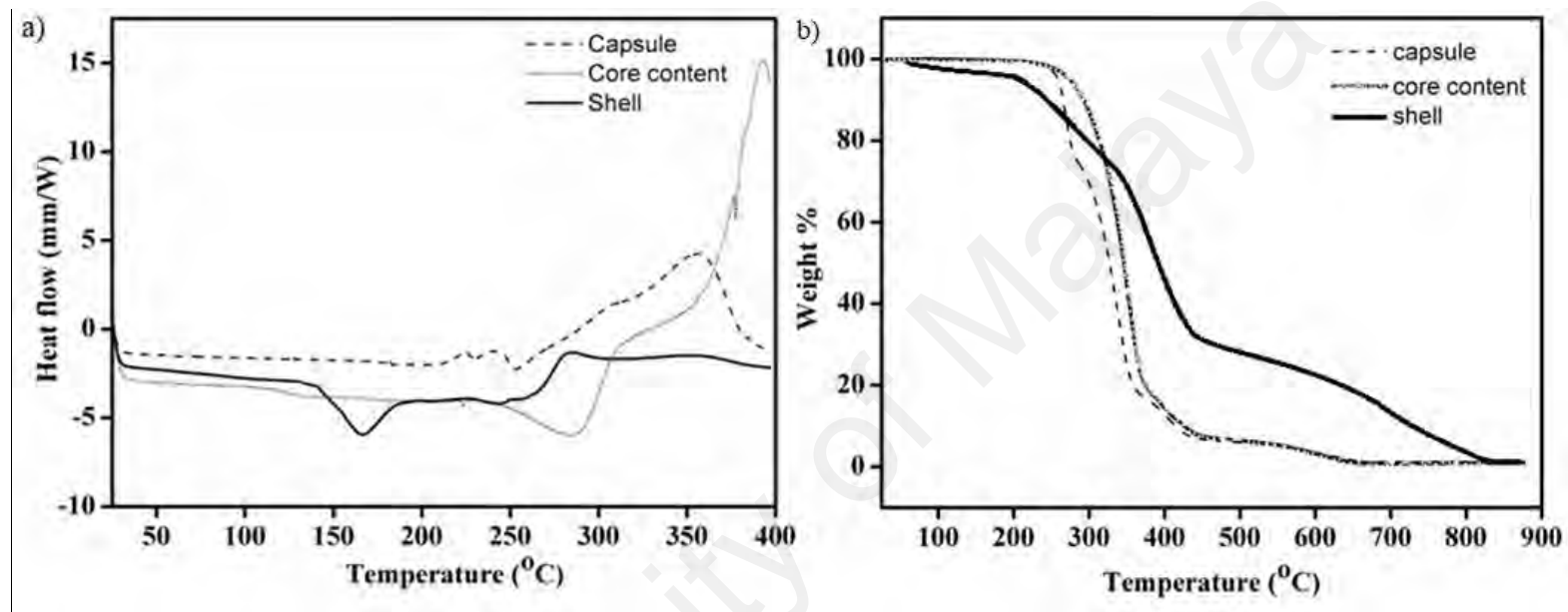


**Figure 4.13:** (a) DSC thermograms and (b) TGA thermograms; of EPON828 microcapsule, separated core and shell materials

(b) *PETMP microcapsule*

Figure 4.14 (a) shows the thermogram of DSC curves of PETMP capsule after being soaked in N,N-dimethylbenzylamine as well as separated core content. The PETMP capsule was soaked in N,N-dimethylbenzylamine which used as catalyst to allow the diffusion of the catalyst into the capsule. Temperature observed at 101.8 °C corresponds to  $T_g$  of PETMP microcapsule while temperature beyond 172 °C attributed to the melting endothermic of microcapsule. Thus, it proposes that this self-healing microcapsule system is stable and suitable to be used at ambient temperature up to < 100 °C owing to high melting and glass transition of the microcapsule.

Figure 4.14 (b) shows the TGA curves of microcapsule soaked in N,N-dimethylbenzylamine, extracted core and separated shell material. Temperature around 180 °C shows a minimum weight loss of 5.5% which attributed to the loss of N,N-dimethylbenzylamine as its boiling point is reported to be around 183-184 °C (Sigma Aldrich, 2012). Since N,N-dimethylbenzylamine is used as catalyst, thus its presence is importance to indicate that this catalyst will remain in the capsule during the embedment of the capsule into the coating matrix. This catalyst takes part in the self-healing reaction. The boiling point of PETMP is reported to be approximately 275 °C. Thus, a sharp drop beyond 300 °C was identified as the evaporation of exuded PETMP (Sigma Aldrich, 2015).

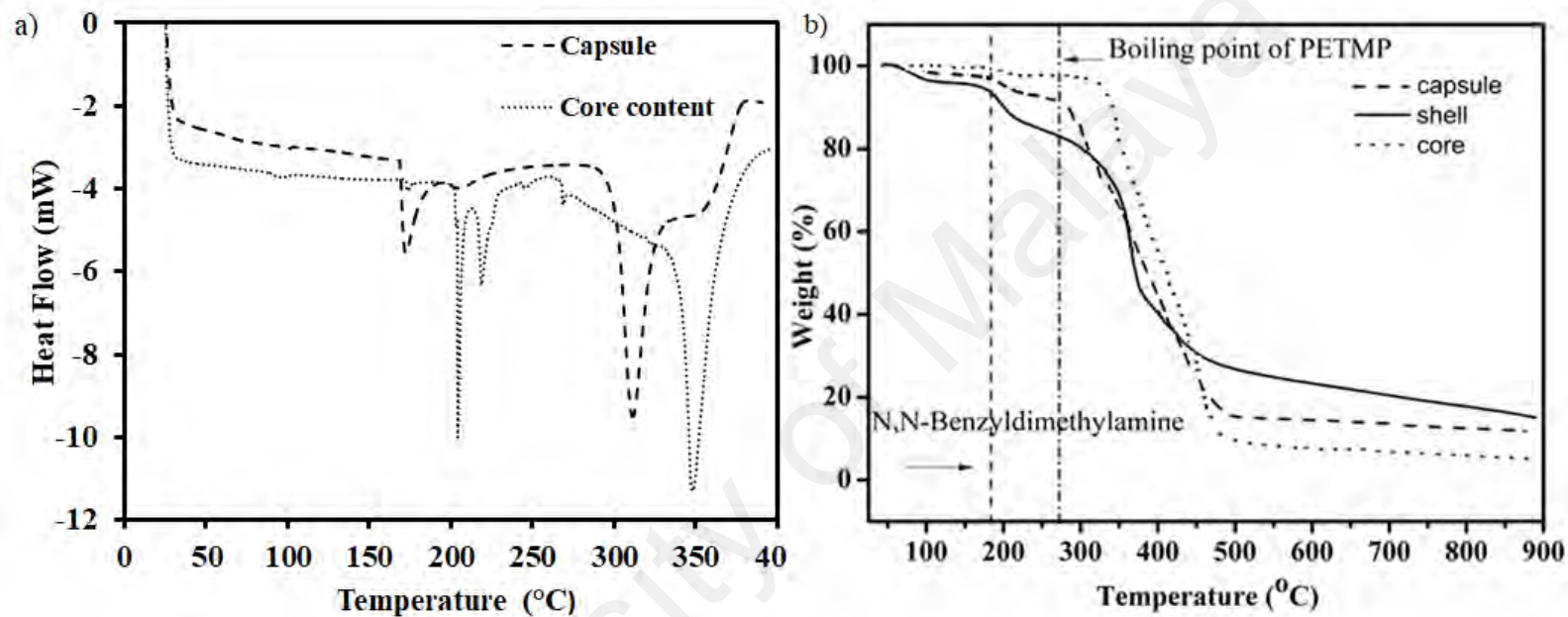


**Figure 4.14:** (a) DSC thermograms and (b) TGA thermograms; of PETMP/N,N-dimethylbenzylamine microcapsule, separated core and shell materials

#### **4.4 Coating mixture preparation**

Alkyd coating mixture was prepared in accordance to Ang work in which the ratio used of MMA: alkyd was 2 parts: 3 parts. MMA which acts as reactive diluents provide  $-C=C-$  in the system. Higher unsaturation in the system will increase the rate of UV curing since the  $-CH=CH-$  provide a site for crosslinking propagation. Thus, it will reduce the tack-free time. However, the ratio of alkyd used should not too low as it must be able to form a continuous film and will improve the dispersion of microcapsules when added and apply on a substrate. Despite that, the mixture of MMA/alkyd should not be too viscous as the coating mixture with low viscosity will improve the diffusion control of free radicals in the systems and thus increase the rate of UV curing. Hence, the ratio of 2 parts MMA: 3 parts alkyd was chosen as it is suitable for coating application. Benzophenone was used as UV photoinitiator instead of other more reactive photoinitiator. Low reactivity of benzophenone ensures that the coating has higher stability and improves its lifespan before being cured (Ang, 2012).

The percentage of microcapsule added in the coating matrix was related to the adhesion strength to the substrate and the efficiency of self-healing ability. Investigation of self-healing reaction on the coating with various loading of microcapsule has been conducted. The investigation was discussed in section 4.4.1 and section 4.4.2.

##### **4.4.1 Evaluation of amount of loading microcapsules on self-healing ability**

Three self-healing coatings with different total amount of microcapsules were prepared (3.0, 5.0 and 7.0 wt %) and were intentionally scratched to initiate the self-healing reaction. All the coatings were observed under calibrated digital microscope (AnMo Electronics, Taipei, Taiwan) to determine the self-healing ability. Generally, the higher the amount of microcapsule in the coating matrix, the better is the

efficiency of self-healing reaction since larger amount of microcapsule present at the damage site. However, the excessive amount of microcapsules loaded into a coating could depreciate some of the physicochemical properties of the coating, especially the film adhesion and the barrier property. When observed under digital microscope, coating with 3.0 and 5.0 wt % loading of microcapsules show no sign of healing reaction due to lack of microcapsule at the damage site (Figure 4.15). Sufficient loading of microcapsule is needed in the coating matrix for the coating to be able to self-heal. Figure 4.16 show the damaged area of coating (7.0 wt%) when observed under digital microscope. Within 3 mins, core content from ruptured microcapsules filled the crack. It can be inferred that 7.0 wt % of microcapsule in the alkyd coating is the sufficient loading amount needed for self-healing reaction.



**Figure 4.15:** Image of simulated scratch of the coating with 5.0 wt% loaded microcapsules.

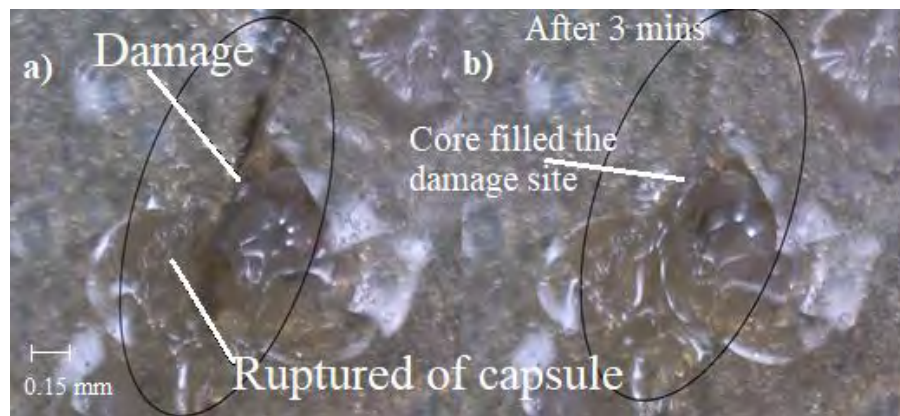


**Figure 4.16:** Image of simulated scratched of self healing coating (a) captured immediately after scratched (b) captured after 3 mins of scratched

#### 4.4.2 Effect of amount of microcapsules on adhesion properties of film on the substrate.

The adhesion properties of coating film on the substrate were investigated with different loading of microcapsules which consists of 7.0, 9.0, 11.0, 13.0 and 15.0 wt%. Table 4.5 shows the relation of loading of microcapsules with the adhesion strength to the substrate. Note that the test was carried out immediately after scribed. Although increase in the amount of microcapsules in the coating may favour the self-healing process, it may at the same time reduce the adhesion strength of the coating matrix to the substrate. Thus, the adhesion test was performed on the coating with higher loading of microcapsule to determine the limit of the loading of microcapsules. From the table, the adhesion strength of the coating to the substrate started to deteriorate with 13.0 wt% loading and onwards. Hence, coating matrix with 7.0 wt% microcapsules was used in the following experiments as this loading shows excellent adhesion strength as well as minimum amount of microcapsules required for the coating to be able to self-heal. By introducing the minimal but sufficient amount of microcapsules, the proportion of natural content of the coating, i.e. palm oil based

alkyd would be relatively high, and this is important especially nowadays when most of the industries are supporting the call for green coatings.

**Table 4.5:** Adhesion strength of coating film

Loading of microcapsule (%)	Film adhesion grade	Film removal
7.0	5A	None
9.0	4A	Trace along incision
11.0	4A	Trace along incision
13.0	3A	<1.6mm along incision
15.0	3A	<1.6mm along incision

#### 4.5 Crosslinked reaction between EPON828 and PETMP

In the reaction between EPON 828 and PETMP, the crosslinking occur between epoxy group from EPON 828 and thiol group from PETMP in the presence of N,N-dimethylbenzylamine as catalyst.

In order to estimate the healing reaction time, the reaction between neat PETMP and neat EPON 828 was analysed by physical inspection and FTIR analysis. The FTIR analysis was performed periodically as the healing agents crosslinked. The healing agents took approximately 10 minutes to harden as it crosslinked when examined physically. This result is in agreement with FTIR analysis. Figure 4.17 shows FTIR spectra of the crosslinking of the healing agents throughout the time. Peak at  $830\text{ cm}^{-1}$  represent epoxy ring stretching of EPON 828. Upon mixing, the intensity peak starts to decrease gradually and disappear completely after 9 mins, as shown in Figure 4.18



(c). The presence of tertiary amine base-catalyst resulted in ring opening of epoxy group, thus reduce the peak intensity of FTIR spectra with increasing time.

The same pattern was also observed for S-H vibration peak of PETMP. The intensity of peak at  $2571\text{ cm}^{-1}$  shown in Figure 4.18 (b) has gradual reduction with increasing time. At 9 mins, the peak almost disappeared. This is due to the breaking of S-H bond owing to the nucleophilic substitution by epoxide anion (Konuray *et al.*, 2017). The reaction between thiols and epoxy group also resulted in increment of peak at  $3500\text{ cm}^{-1}$  which represent O-H stretching. The result of epoxy-thiols reaction forming hydroxyl can be observed at peak  $3500\text{ cm}^{-1}$  and shown in Figure 4.18 (a).

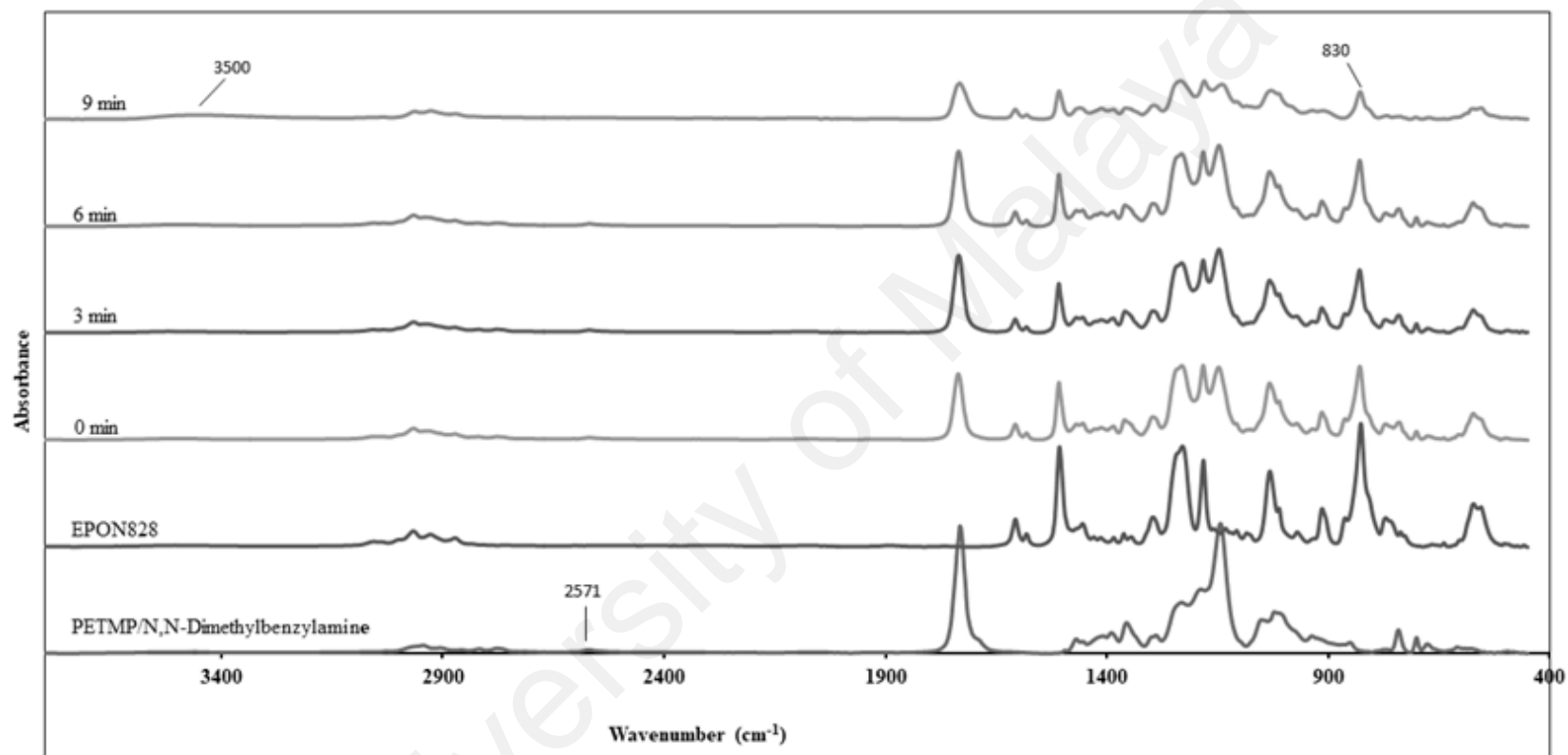


**Figure 4.17:** FTIR spectra of reaction between EPON828 and PETMP at different time intervals

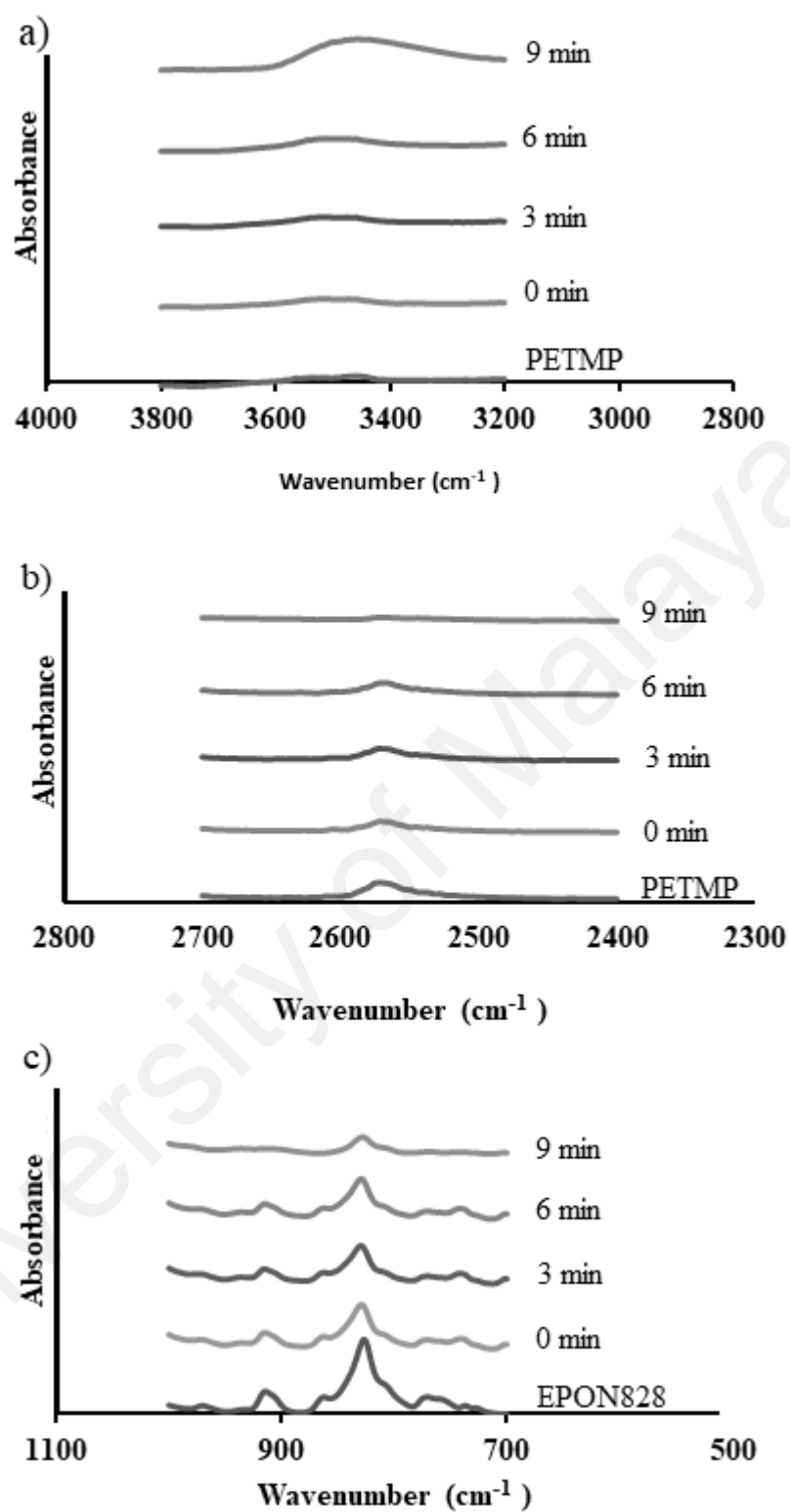


**Figure 4.18:** Assignment peaks of FTIR spectrum of PETMP-EPON828 crosslinked (a) hydroxyl peak, (b) thiols peak, and (c) epoxy peak

#### 4.6 Coating film properties

In the adhesion test, the control alkyd and self healing coating show excellence performance as no depreciation observed. Note that the adhesion test was conducted immediately after the X-cut was done on the coating without undergo self healing. Film adhesion test was also conducted on the coating after the coating has self healed. Similar result was also observed as no depreciation observed. All the coating were recorded film adhesion with grade 5A.

The result of adhesion, water, alkali, acid and salt water resistance test was summarised in Table 4.6. In water resistance test, both coating shows excellence resistance towards water. The whitening formed after 24 hours immersion in water were disappear within 1 hour after removed from the immersion. The maleated alkyd coating is known to have high resistance towards water due to higher amount of  $-\text{CH}=\text{CH}-$  from maleic acid (Ang, 2012). Even with the addition of microcapsules, the alkyd coating also does not depreciate the coating resistivity towards water. Similar case was also observed in acid and saltwater test. Both coatings show no visual defect after removed from immersion of aqueous HCl and NaCl solution. In contrary, both coatings show film defect after removed from the immersion NaOH aqueous solution indicate that both coatings has low resistivity towards alkali solution. In less than 1 hour of immersion, the coatings already show film detachment. This is due to the hydrolysis of ester linkages in the alkyd.

**Table 4.6:** Physicochemicals properties of coating film

Coating	Water resistance <sup>a</sup>	Alkali resistance / (min) <sup>b</sup>	Acid resistance <sup>a</sup>	Saltwater resistance <sup>a</sup>
Self healing coating	√	<5	√	√
Control alkyd coating	√	<5	√	√

<sup>a</sup> √ = Not affected<sup>b</sup> Time interval of alkali immersion before apparent film defects

## 4.7 Corrosion test

### 4.7.1 Basic corrosion tests

The performance of self healing coating was investigated visually by using digital microscope. Alkyd with 7 wt% of microcapsules was coated onto mild steel and exposed to UV radiation for curing. The mild steel was then intentionally scratched using razor blade. The mild steel was then allowed to self heal and conditioned for 24 hours before it is immersed in 3.5 wt% NaCl solution. Basic corrosion test and visual inspection via digital microscope was performed to evaluate the efficacy of alkyd coating with self healing ability in corrosion protection. Both self healing coating and control alkyd coating were scratched and left for 24 h at room temperature. This was to allow sufficient time for the healing agents to properly fill up the cracked plane. The samples were then immersed in 3.5 wt% of NaCl solution for 24 hours before evaluating the condition of the coating near the damaged site under digital microscope. Figures 4.19 (a) and (b) show the image of the self healed coating before and after immersion in NaCl solution. There is no apparent sign of corrosion at the test area. Figure 4.19 (c) and (d) shows similar comparison for control alkyd coating (without

any loaded microcapsules), and there is obvious corrosion taking place along the crack.

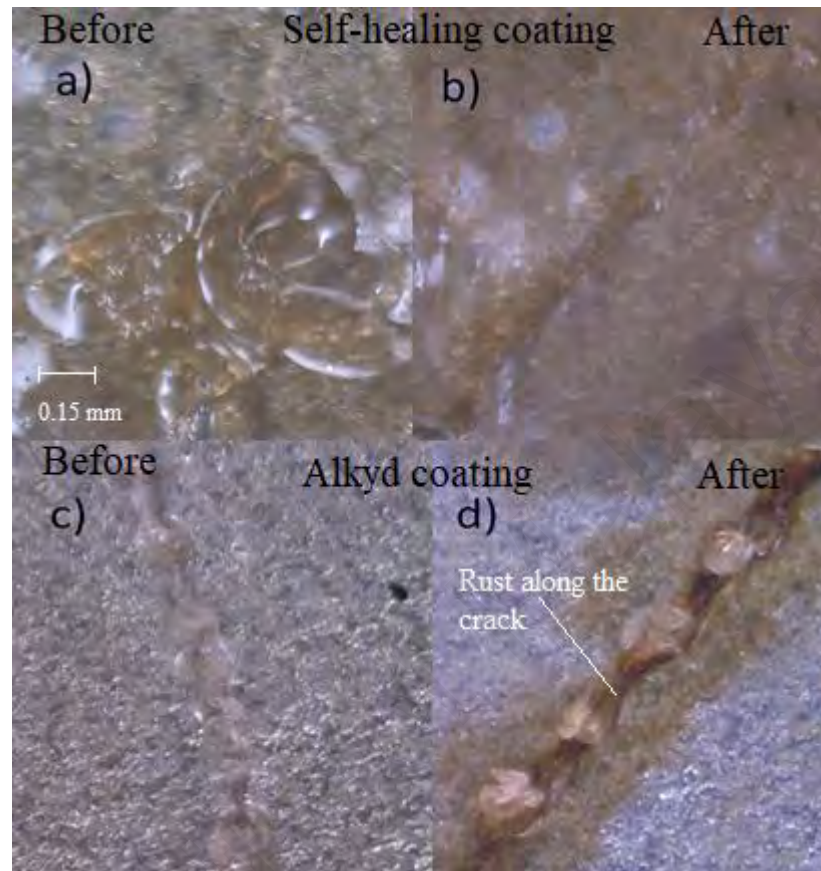


**Figure 4.19:** Self healed coating (a) before immersed in NaCl solution, (b) after one day immersion in NaCl solution; control alkyd coating (c) before immersed in NaCl solution, and (d) after one day immersion in NaCl solution

#### 4.7.2 Potentiodynamic polarization experiment

Electrochemical corrosion studies were conducted to investigate the corrosion protection ability of the self-healing alkyd coating, and also to complement the basic corrosion experiment above. The result of potentiodynamic polarization experiment is shown in Figure 4.20. The extrapolation of Tafel region shows that both self-healing coating after scribe (coating SH-AS), and before scribe (coating SH-BS) has lower  $i_{corr}$  values compared to control alkyd coating with scribe (coating A). The lower  $i_{corr}$  signify that both self-healing coatings, SH-AS and SH-BS have lower corrosion current density compared to the control, coating A. For clarification, self-healing coating after scribe, coating SH-AS refers to self-healing coating that has been scribed and allowed to self-heal, while coating before scribe, SH-BS refers to undamaged self-healing coating. As for the control, coating A, it refers to alkyd coating without loaded microcapsules (i.e. without self-healing ability) and has been scribed. The relatively low  $i_{corr}$  value indicates that the self-healing coatings are able to provide prolonged corrosion protection to the metal substrate. Since the  $i_{corr}$  value of self-healing coating with scribe is comparable with self-healing coating without scribe, it is presumed that the coating has self-healed sufficiently to the state before damage incurred and continue provide protection to the substrate (Yogandan *et al.*, 2015). This event reveals that the healing agents (EPON828 and PETMP) was released from the ruptured microcapsules, filled the damaged site (scribed area) and undergo crosslinking to form a protective layer. Since the damaged area was protected from the aggressive corrosion attack, the alkyd coating with self-healing ability is able to provide prolonged corrosion protection to the substrate.

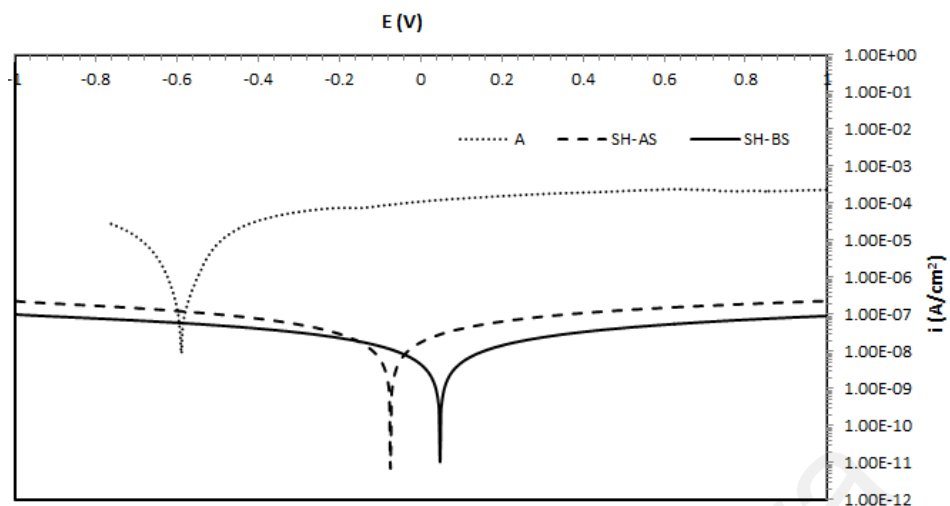


**Figure 4.20:** Polarization curves of coating samples after 3 hours in contact with 3.5 wt% NaCl.

Table 4.7 shows the results of corrosion rate analysis. The results in Table 4.7 show that coating A has higher corrosion rate compared to the other two coatings. As the corrosion rate of coating SH-AS is comparable with coating SH-BE, the presence of microcapsules in the alkyd coating that provide self-healing properties has undeniably improved the coating ability to provide prolonged corrosion protection, and eventually increase the lifespan of the substrate.

**Table 4.7:** Polarization results after immersion in 3.5 wt% NaCl.

Coating	$E_{corr}$ , (V)	$i_{corr}$ (A/cm <sup>2</sup> )	Corrosion rate (mm/year)
A	-0.5829	$1.653 \times 10^{-6}$	$1.921 \times 10^{-2}$
SH-AS	-0.0731	$7.001 \times 10^{-9}$	$8.135 \times 10^{-5}$
SH-BE	0.0491	$2.841 \times 10^{-9}$	$3.302 \times 10^{-5}$



## **CHAPTER 5: CONCLUSION AND RECOMMENDATIONS**

### **5.1 Conclusion**

UV-curable alkyd coating with self-healing ability was successfully synthesized by embedding microcapsule containing healing agents (EPON828 and PETMP in the presence of catalyst) into the alkyd coating. The simulated damage of the coating was successfully healed upon the crosslinking of healing agents as they exude out from the ruptured capsules and filled the damage site. The propagation of crack itself is a driving force for the microcapsule to rupture. 7% loaded microcapsules in the coating was found to be the minimal but sufficient for the coating to be able to self-heal.

Result from the corrosion study shows that the scribed self-healing alkyd (SH-AS) coating has lower corrosion rate as compared to scribed alkyd coating (A) without self-healing ability. This is owing to the scribed area of SH-AS coating was self-healed upon crosslinking, thus the surface of the substrate was covered and protected against corrosive attacked. Hence, self-healing properties provide protection for the substrate against corrosion which eventually increases the lifespan of the substrate. In fact the result also shows that the corrosion rate of SH-AS was similar with SH-BS coating. The SH-BS coating is the coating of self-healing without scribe.

The film properties of self-healing coating are similar to alkyd coating (without microcapsule). Both coatings show excellence performance except in the test of alkali resistance. In the alkali resistance test, both coatings show depreciation due to hydrolysis of ester linkages. Thus, the introduction of microcapsules into the coating does not depreciate the film properties of the coating.

### **5.2 Recommendation for Future Study**

In this study, the self-healing ability of the alkyd coating was investigated at the larger scale damage of the coating. The scratch was incurred on the alkyd coating with

bigger and deeper damage for it to be able being investigated for the self-healing ability of the coating externally with the instruments and technology provided. Since this research is a preliminary success, the investigation of self-healing ability that occurs at the internal damage of the coating may be conducted. The presence of internal damage on the coating such as the formation of microcracks when left unattended may result in severe impairment to the coating and thus result in damage to the substrate. Hence, the study of self-healing ability on the internal damage of the coating is important before being transferred into industrial application.

Besides that, we investigated the commercial epoxy as one of the healing agents in this study. Thus in the future work, it would be an interesting when investigation of the potential of epoxy from epoxidized vegetable oil as one of the healing agents could be done. The epoxidized vegetable oil serves as an alternative to the commercial epoxy which is EPON828. In addition, this type of epoxy added value towards more environmental friendly research development and much more cost effective.

In this study, thiols have been used as the epoxy hardener. Since thiol is very reactive due to the presence of hydrosulfide group, it requires more robust polymer to encapsulate it. Thus, the study of the substitute to this type of epoxy hardener can address the difficulty of encapsulation process in future work.

## REFERENCES

- Aïssa, B., Therriault, D., Haddad, E., & Jamroz, W. (2012). Self-healing materials systems: Overview of major approaches and recent developed technologies. *Advances in Materials Science and Engineering*, 2012, 1-17.
- Ali, K. I., Khan, M. A., Zaman, M. M., & Hossain, M. A. (1994). Reactive diluent effect on properties of UV-cured films. *Journal of Applied Polymer Science*, 54(3), 309–315.
- Ang, D. T. C. (2012). *Conversion of non self-drying palm stearin alkyd into environmental friendly ultraviolet-curable resin* (PhD thesis, University of Malaya, Kuala Lumpur).
- Ang, D. T. C. (2015). Effect of reactive diluent on physicochemical and thermal properties of UV-curable alkyd coatings. *Journal of Coating Technology and Research*, 1-8.
- Ang, D. T. C., & Gan, S. N. (2012a). Development of palm oil-based alkyds as UV curable coatings. *Pigment and Resin Technology*, 41(5), 302-310.
- Ang, D. T. C., & Gan, S. N. (2012b). Novel approach to convert non-self drying palm stearin alkyds into environmental friendly UV curable resins. *Progress in Organic Coating*, 73(4), 409-414.
- Ang, D. T. C., Khong, Y. K., & Gan, S. N. (2013). Novel approach to enhance film properties of environmentally friendly UV-curable alkyd coating using epoxidised natural rubber. *Progress in Organic Coatings*, 76(4), 705-711.
- Barcelos, E., Rios, S. de A., Cunha, R. N. V., Lopes, R., Motoike, S. Y., Babiychuk, E., ... Kushnir, S. (2015). Oil palm natural diversity and the potential for yield improvement. *Frontiers in Plant Science*, 6(190), 1-16.
- Bentivoglio, D., Finco, A., & Bucci, G. (2018). Factors affecting the Indonesian palm oil market in food and fuel industry: Evidence from a time series analysis. *International Journal of Energy Economics and Policy*, 8(5), 49-57.
- Bhargava, G., & Allen, F. (2012). Self-healing, chromate-free conversion coating for magnesium alloys. *Metal Finishing*, 110(4), 32-38.
- Blaiszik, B. J., Caruso, M. M., McIlroy, D. A., Moore, J. S., White, S. R., Sottos, N. R., (2009). Microcapsules filled with reactive solutions for self-healing materials. *Polymer*, 50(4), 990-997.
- Brown, E. N., White, S. R., Sottos, N. R. (2004). Microcapsule induced toughening in a self-healing polymer composite. *Journal of Material Science*, 39(5), 1703-1710.
- Chiplunkar, P. P., & Pratap, A. P. (2016). *Utilization of sunflower acid oil for synthesis of alkyd resin*. *Progress in Organic Coatings*, 93, 61–67.

- Cho, S. H., Andersson, H. M., White, S. R., Sottos, N. R., Braun, P. V. (2006). Polydimethylsiloxane-based self-healing materials. *Advanced Materials*, 18(8), 997-1000.
- Cho, S. H., White, S. R., Sottos, Braun, P. V. (2009). Self-healing polymer coatings. *Advanced Materials*, 21(6), 645-649.
- Dietrich, K., Bonatz, E., Nastke, R., Herma, H., Walter, M., & Teige, W. (1990). Amino resin microcapsules: IV. Surface tension of the resins and mechanism of capsule formation. *Acta Polymerica*, 41(2), 91-95.
- Dry, C. (1996). Procedures developed for self-repair of polymer matrix composite materials. *Composite Structure*, 35(3), 263-269.
- Duan, B. (2016). Microencapsulation via in situ polymerization. In M. Mishra, *Handbook of Encapsulation and Controlled Release* (pp. 307-311). Boca Raton: Taylor & Francis Group.
- Ghosh, S. K. (2006). *Functional Coatings: By Polymer Microencapsulation*. Weinheim: Wiley-VCH Verlag GmbH & Co. KGaA.
- Ghosh, S. K. (2009). *Self-healing materials: fundamentals, design strategies, and applications*. Weinheim: Wiley-VCH Verlag GmbH & Co. KGaA.
- Giro-Paloma, J., Martínez, M., Cabeza, L. F., & Fernández, A. I. (2016). Types, methods, techniques, and applications for microencapsulated phase change materials (MPCM): A review. *Renewable and Sustainable Energy Reviews*, 53, 1059-1075.
- Glöckner, P., Jung, T., Struck, S., & Studer, K. (2008). *Radiation Curing*. Hannover: Vincentz Network GmbH & Co KG.
- Gorkum, V. R., & Bouwman, E. (2005). The oxidative drying of alkyd paint catalysed by metal complexes. *Coordination Chemistry Reviews*, 249(17), 1709-1728.
- Guner, F. S., Yagci, Y., & Erciyes, A. T. (2006). Polymers from triglyceride oils. *Progress in Polymer Science*, 31(7), 633-670.
- Gündüz, G. (2016). *Chemistry, materials, and properties of surface coatings: Traditional and Evolving Technologies*. Pennsylvania: DEStech Publications.
- Hamdy, A. S., Doench, I., & Möhwald, H. (2011). Smart self-healing anti-corrosion vanadia coating for magnesium alloys. *Progress in Organic Coatings*, 72(3), 387-393.
- Heitkamp, A., & Pellowe, D. (1995). Alkyd and Polyesters. In Koleske, J. V., *Paint and coating testing manual* (53-59). Philadelphia: American Society For Testing Materials.
- Holmberg, K. (2001). Alkyd Resins. In D. Satas, & A. A. Tracton, *Coatings Technology Handbook* (pp. 435-443). USA: Marcel Dekker.

- Holmberg, K. (2006). Alkyd Resins. In A. A. Tracton, *Coatings Materials and Surface Coatings*, 6-1 - 6-11. Boca Raton: Taylor & Francis Group.
- Isaac, I. O., & Nsi, E. W. (2013). Influence of polybasic acid type on the physicochemical and viscosity properties of cottonseed oil alkyd resins. *The International Journal of Engineering And Science*, 2(5), 1-14.
- Islam, M. R., Beg, M. H., & Jamari, S. S. (2014). Alkyd based resin from non-drying oil. *Procedia Engineering*, 90, 78-88.
- Issam, A. M., & Cheun, C. Y. (2009). A study of the effect of palm oil on the properties of a new alkyd resin. *Malaysia Polymer Journal*, 4, 42-49.
- Jones, F. N., Nicholas, M. E., & Pappas, S. P. (2017). *Organic Coatings: Science and Technology*. USA: John Wiley & Sons.
- Koch, G., Varney, J., Thompson, N., Moghissi, O., Gould, M., & Payer, J. (2016). *International measures of prevention, application, and economic of corrosion technologies study*. Retrieved from <http://impact.nace.org/economic-impact.aspx>
- Konuray, , A. O., Ramis, X., & Fernández-Francos, X. (2017). Analysis of the reaction mechanism of the thiol–epoxy addition initiated by nucleophilic tertiary amines. *Polymer Chemistry*, 8, 5934-5947.
- Lambourne, R. (1999). Paint composition and applications-a general introduction. In R. Lambourne, & T. A. Strivens, *Paint and surface coatings: Theory and practice* (pp. 1-18). England: Woodhead Publishing Ltd.
- Lanson, H. J. (1985). Chemistry and technology of alkyd and saturated reactive polyester resins. *Applied Polymer Science*, 1181-1204.
- Malaysian palm oil industry (2011). Retrieved 26, August , 2018 from [http://www.palmoilworld.org/about\\_malaysian-industry.html](http://www.palmoilworld.org/about_malaysian-industry.html) )
- Manea, M. (2008). *High Solid Binders*. Hannover: Vincents Network GmbH
- Marrion, A. R. (2004). *The Chemistry and Physics of Coatings*. UK: The Royal Society of Chemistry.
- McIntyre, J. E. (2003). The Historical Development of Polyesters. In J. Scheirs, & T. E. Long, *Modern Polyesters: Chemistry and Technology of Polyesters and Copolyesters* (pp. 3-18). England: John Wiley & Sons Ltd.
- Miranda, T. J. (1993). The Future of the Coatings Industry. In Oil and Colour Chemists' Association, *Surface Coatings: Volume 1 Raw Materials and Their Usage* (pp. 1-10). Dordrecht: Springer Science+Business Media.
- Misev, T., & van der Linde, R. (1998). Powder coatings technology: new developments at the turn of the century. *Progress in Organic Coatings*, 34(1-4), 160–168.

- Moake, J. L. (2016). How Blood Clots (Consumer version). Retrieved on 31/5/2016 from <http://www.msmanuals.com/home/blood-disorders/blood-clottingprocess/how-blood-clots>
- Momentive. (2015). EPON828, Material Safety Data Sheet. Retrieved on 2017 from <http://gato-docs.its.txstate.edu/jcr:7e57559a-d250-4298-8386-8eda1fca3517/epon+resin+828.pdf>
- Palanikkumaran, M., Gupta, K. K., Agrawal, A. K., & Jassal, M. (2009). Highly stable hexamethylmelamine microcapsules containing n-octadecane prepared by in situ encapsulation. *Journal of Applied Polymer Science*, 114(5), 2997-3002.
- Samadzadeh, M., Boura, S. H., Peikari, M., Kasiriha, S. M., & Ashrafi, A. (2010). A review on self-healing coatings based on micro/nanocapsules. *Progress in Organic Coatings*, 68(3), 159–164.
- Sigma Aldrich. (2012). N,N-Dimethylbenzylamine, Material Safety Data Sheet. Retrieved on 2017 from <http://www.sigmaaldrich.com/catalog/product/aldrich/185582?lang=en&region=MY>.
- Sigma Aldrich (2015). Pentaerythritol tetrakis(3-mercaptopropionate), Material Safety Data Sheet. Retrieved on 2017 from <http://www.sigmaaldrich.com/catalog/product/aldrich/381462?lang=en&region=MY>.
- Schwalm, R. (2007). *UV coatings: Basics, recent development and new applications*. UK: Elsevier.
- Somani, K. P., Kansara, S. S., Patel, N. K., & Rakshit, A. K. (2003). Castor oil based polyurethane adhesives for wood-to-wood bonding. *International Journal of Adhesion*, 23(4), 269-275.
- Sørensen, P. A., Kiil, S., Dam-Johansen, K., & Weinell, C. E. (2009). Anticorrosive coatings: a review. *Journal of Coating Technology and Research*, 6(2), 135-176.
- Stankiewicz, A., Szczygieł, I., & Szczygieł, B. (2013). Self-healing coatings in anti-corrosion applications. *Journal of Materials Science*, 48(23), 8041-8051.
- Stansbury, E. E., & Buchanan, R. A. (2000). *Fundamentals of Electrochemical Corrosion* (pp. 147-149). USA: ASM International.
- Stoye, D., & Freitag, W. (1998). *Paints, Coatings and Solvents*. New York: Wiley-VCH Verlag GmbH.
- Suryanarayana, C., Rao, K. C., & Kumar, D. (2008). Preparation and characterization of microcapsules containing linseed oil and its use in self-healing coatings. *Progress in Organic Coatings*, 63(1), 72-78.

- Tan, C. P., & Nehdi, I. A. (2012). The physicochemical properties of palm oil and its components. *Palm Oil*, 377–391.
- Tiwari, A., Galanis, A., & Soucek, M. D. (2016). *Biobased and environmentally benign coatings*. John Wiley & Sons.
- Teoh, C.H. (2002). *The Palm Oil Industry in Malaysia: From Seed to Frying Pan*. Report of WWF, Malaysia
- Weiss, K. D. (1997). Paint and coatings: A mature industry in transition. *Progress in Polymer Science*, 22(2), 203–245.
- White, S. R., Sottos, N. R., Geubelle, P. H., Moore, J. S., Kessler, M., Sriram, S. R., ... & Viswanathan (2001). Autonomic healing of polymer composites. *Nature*, 409(6822), 794–797.
- Wicks, Z. W. (2002). Alkyd Resins (Vol. 2). *Kirk-Othmer Encyclopedia of Chemical Technology*. New Jersey, US: John Wiley & Sons.
- Yogandan, G., Pradeep, P. K., & Balaraju, J. N. (2015). Evaluation of corrosion resistance and self-healing behavior of zirconium–cerium conversion coating developed on AA2024 alloy. *Surface Coating and Technology*, 270, 249-258.
- Yuan, Y. C., Rong, M. Z., Zhang, M. Q., Chen, J., Yang, G. C., & Li, X. M. (2008). Self-healing polymeric materials using epoxy/mercaptan as the healant. *Macromolecules*, 41(14), 5197-5202.
- Zhang, M. Q., & Rong, M. Z. (2011). *Self-Healing Polymers and Polymer Composites*. John Wiley & Sons.

## LIST OF PUBLICATIONS AND PAPERS PRESENTED

### List of publication

1. **Saman, N. M.**, Shahabudin, N., Gan, S. N., Basirun, W. J., & Ang, D. T. C. (2018). UV-Curable alkyd coating with self-healing ability. *Journal of Coatings Technology and Research*, 1-12.
2. **Saman, N. M.**, Ang, D. T. C., & Gan, S. N. (2018). Acrylated epoxidized soybean oil as a green alternative healant in development of autonomous self-healing materials. *Journal of Polymers and the Environment*, 27(1), 118-126.

### List of conference

1. UM-NTU Bilateral Symposium on Advanced Materials (Aug 2018), University of Malaya, Kuala Lumpur, Malaysia.